Erstgutachterin: PD Dr. Jeanette Lorenz
Zweitgutachter: Prof. Dr. Wolfgang Dünnweber

Search for electroweakinos with the ATLAS detector

Thesis submitted for a doctoral degree in physics
at the faculty of physics of the
Ludwig-Maximilians University
Munich, Germany

Submitted by Eric Schanet, born in Luxembourg
on May 4th, 2021

Supported by the Luxembourg National Research Fund (FNR) (13562317)

Part I

Fundamental concepts

Part II

The 1-lepton analysis

Chapter 6

Background estimation

A reliable and trustworthy estimation of the expected Standard Model (SM) background rates in the signal regions is crucial for exercising the statistical machinery, laid out in chapter 3, and making conclusive statistical statements about the Supersymmetry (SUSY) scenarios studied. The background estimation approaches used herein rely on semi-data-driven techniques or purely on Monte Carlo (MC) estimations. As estimating backgrounds only from MC simulation is sometimes problematic, e.g., due to mis-modelings in the phase space targeted not appropriately covered by the uncertainties, a (semi-)data-driven approach is often favoured. In the following, the major backgrounds $t\bar{t}$, single top and W + jets are estimated using a semi-data-driven approach, while the expected rates from the remaining, smaller backgrounds purely rely on MC simulations and are normalised to their theoretical cross sections.

6.1 General strategy

6.1.1 Transfer factor approach

Estimating background contributions in signal regions (SRs) in a semi-data-driven approach usually involves the introduction of so-called control regions (CRs), used to control dominant background processes by comparing their expected event rates to data. The CRs are designed to be enriched in events of a given background process (or type) while being approximately free of signal contamination. If $N_p^{\mathrm{MC}}(\mathrm{SR})$ and $N_p^{\mathrm{MC}}(\mathrm{CR})$ are the expected rates for a given background process p obtained from MC simulation in a given SR and CR, respectively, then the transfer factor $N_p^{\mathrm{MC}}(\mathrm{SR})/N_p^{\mathrm{MC}}(\mathrm{CR})$ allows to convert the number of observed background events in the control region, $N_p^{\mathrm{obs.}}(\mathrm{CR})$, into a background estimate in the signal region, $N_p^{\mathrm{est.}}(\mathrm{SR})$, through

$$N_p^{\mathrm{est.}}(\mathrm{SR}) = N_p^{\mathrm{obs.}}(\mathrm{CR})\frac{N_p^{\mathrm{MC}}(\mathrm{SR})}{N_p^{\mathrm{MC}}(\mathrm{CR})} = \mu_p N_p^{\mathrm{MC}}(\mathrm{SR}). \tag{6.1}$$

Here, μ_p is the process-specific normalisation factor introduced in section 3.1. An important benefit of this approach is that the impact of systematic uncertainties on the estimated background rates can be evaluated on the transfer factors, i.e. ratios of MC estimates. As such, systematic uncertainties can partly cancel in the extrapolation to the SRs. The uncertainty on the background estimate in the SRs is

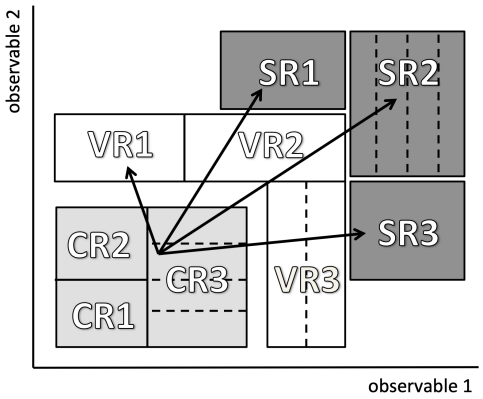

Figure 6.1: Schematic view of an analysis strategy including multiple control, validation and signal regions with one or multiple bins each. Extrapolations from the control regions into the signal regions can be verified in the validation regions lying in the phase space extrapolated over. All regions are designed to be statistically independent. Figure adapted from Ref. [169].

then a combination of the statistical uncertainties in the CRs, the uncertainties on the normalisation factors, and remaining uncertainties affecting the extrapolation [169].

As indicated in eq. (6.1), the transfer factor approach is formally equivalent to using the process-specific normalisation factors from section 3.1, effectively *normalising* the number of total background events expected from MC simulation to the number of observed events in each control region. Multiple disjoint CRs are used to simultaneously normalise multiple background processes to data in a combined fit. In order not to have an underdetermined minimisation problem, the number of CRs needs to be at least as large as the number of normalisation factors considered. Two different profile likelihood fit configurations are used in the following; the first configuration being a so-called *background-only* fit configuration, assuming no signal contribution and typically only including the CRs. The second configuration is a so-called *signal-plus-background* fit configuration considering signal contribution and including all CRs as well as SRs (therefore also sometimes called a *model-dependent* fit configuration).

In order to verify the quality of the extrapolation from the CRs to the SRs, so-called validation regions (VRs) are defined. VRs do not participate in the actual fit of the model parameters to data, but serve as intermediate regions to verify the extrapolation. For this reason, VRs are typically placed in the region between the CRs and SRs that is extrapolated over. A schematic view of an analysis strategy using all three types of regions is shown in fig. 6.1. All three types of regions can have more than one bin and are separated by means of suitable observables that are extrapolated over. In order to be able to use information from all control and signal regions in a single profile likelihood fit, all regions necessarily need to be statistically independent.

6.1.2 Analysis blinding

An important concept in the design phase of searches for new physics is the idea of *blinding* regions of interest [251], meaning that measured data are not looked at in these regions. This avoids issues of *experimenter's bias*, i.e. unintended influences on the design of the analysis based on the observed data. If data were already known when designing the signal regions (and therefore the outcome of the analysis would be known to some extent), experimenter's bias could for example occur during the selection of the final signal region definitions.

During the design of a search for SUSY, signal regions are generally kept blinded until the complete analysis strategy is fixed. Once the SRs have been designed, the next step is to develop a suitable

background estimation strategy, often involving the introduction of CRs with negligible signal contamination. This is then often followed by the design of VRs that can be unblinded once the CRs are fixed. After the extrapolation of the background estimate (obtained using a background-only fit) from the CRs has been verified in the VRs, the SRs are unblinded, allowing to quantify potential excesses in data or set limits on model parameters.

6.1.3 Data versus Monte Carlo plots

In this chapter, all plots comparing data versus MC are so-called *pre-fit* plots, meaning that no background-only fit has been run in order to determine the normalisation factors and total systematic uncertainties for the background estimate. Instead, the contributions from the dominant backgrounds $t\bar{t}$, W + jets and single top are normalised simultaneously in the control regions by solving the system of i equations

$$n_{\text{data}}^{\text{CR}_i} = \mu_{t\bar{t}} B_{t\bar{t}}^{\text{CR}_i} + \mu_W B_W^{\text{CR}_i} + \mu_{\text{ST}} B_{\text{ST}}^{\text{CR}_i} + B_{\text{other}}^{\text{CR}_i}, \tag{6.2}$$

where i runs over the list of CRs introduced in section 6.2 and $\mu_{t\bar{t}}$, μ_{W} and μ_{ST} are the normalisation factors of the $t\bar{t}$, W + jets and single top backgrounds, respectively, that are to be determined. $B_{t\bar{t}}^{\text{CR}_i}$, $B_{\text{ST}}^{\text{CR}_i}$, $B_{\text{ST}}^{\text{CR}_i}$ and $B_{\text{other}}^{\text{CR}_i}$ are the background rates expected from MC simulation in the i-th CR. The normalisation factors obtained are 0.96 for $t\bar{t}$, 1.24 for W + jets and 0.73 for single top. As will be shown in section 8.1, the normalisation factors obtained using the full statistical procedure will be close to these values.

Additionally, the uncertainty bands on the background estimate in the plots only include MC statistical as well as experimental uncertainties. The variations of the experimental uncertainties are normalised to the nominal background estimate in the case of $t\bar{t}$, W + jets and single top, such that only the shapes of the dominant backgrounds are affected. For the remaining minor backgrounds, the experimental uncertainties can affect both normalisation and shape. All experimental uncertainties are assumed to be fully correlated over all processes and bins, allowing them to be summed in quadrature. Finally, the uncertainty bars on the data points are obtained by assuming data to be Poisson distributed and correspond to the 68% confidence interval.

6.2 Control regions

The contributions from $t\bar{t}$, W + jets production and single top processes are normalised to data in dedicated control regions. Other processes like Z + jets, diboson and multiboson, $t\bar{t}$ + V, $t\bar{t}$ + h and V + h are estimated directly from MC simulation and normalised to their theoretical cross sections. All CRs are designed to be kinematically as close as possible to the SRs, such that the normalisation factors derived in the CRs are also valid in the SRs. The CRs are mutually exclusive and made orthogonal to the SRs through their requirements on m_{T}, m_{CT} and $m_{b\bar{b}}$. Apart from the requirements on these three observables, as well as the requirement on $m_{\ell b_1}$ (removed altogether in the CRs), the CRs share the same set of cuts as the SRs. Figure 6.4(a) illustrates the configuration of all CRs, especially highlighting the fact that all CRs are located in sideband regions off the $m_{b\bar{b}}$ window, significantly reducing signal contamination. Table 6.1 summarises the kinematic requirements separating the CRs from other regions of interest in the analysis. The pre-fit distributions of all CRs in representative observables are shown in fig. 6.2.

Table 6.1: Overview of the CR and VR definitions. With the exception of $m_{\ell b_1}$, which is not used in the definitions of the CRs and VRs, all regions share the same selection as the SRs on the remaining kinematic observables not listed here.

CR	**TR-LM**	**TR-MM**	**TR-HM**	**WR**	**STR**	
$m_{b\bar{b}}$ [GeV]		<100 or >140		$\in [50, 80]$	>195	
m_{T} [GeV]	$\in [100, 160]$	$\in [160, 240]$	>240	$\in [50, 100]$	>100	
m_{CT} [GeV]		<180		>180	>180	
VR	**VR-onLM**	**VR-onMM**	**VR-onHM**	**VR-offLM**	**VR-offMM**	**VR-offHM**
$m_{b\bar{b}}$ [GeV]		$\in [100, 140]$		$\in [50, 80] \cup [160, 195]$	$\in [50, 80] \cup [160, 195]$	$\in [50, 75] \cup [165, 195]$
m_{T} [GeV]	$\in [100, 160]$	$\in [160, 240]$	>240	$\in [100, 160]$	$\in [160, 240]$	>240
m_{CT} [GeV]		<180			>180	

Control regions for $t\bar{t}$

As events from $t\bar{t}$ processes constitute the dominant SM background in the majority of the SRs, it is necessary to have a precise and reliable estimate of their contributions. Three CRs are defined for $t\bar{t}$, following the same binning in m_{T} as the signal regions, and thus called TR-LM, TR-MM and TR-HM in the following.

A good purity of $t\bar{t}$ processes, as well as the necessary high MC statistics, are achieved by inverting the requirement on m_{CT}, selecting events below the kinematic endpoint for $t\bar{t}$ processes. The achieved pre-fit $t\bar{t}$ purities are 79.6% in TR-LM, 85.9% in TR-MM and 84.1% in TR-HM. The remaining contributions stem mostly from single top and W + jets processes and vary between 8.6%–14.1% and 1.8%–4.3%, respectively, depending on the SR.

For a trustworthy estimate of the contributions from $t\bar{t}$ processes, it is important that the control regions associated to each signal region exhibit approximately the same composition of $t\bar{t}$ decay modes. The decay mode most relevant to the 1ℓ search at relatively low and moderate values of m_{T} is the semi-leptonic decay ($\ell\nu qq$), where one of the W bosons decays leptonically, while the other one undergoes a hadronic decay. The semi-leptonic decay mode exhibits the well-known kinematic endpoint in m_{T} and thus quickly loses importance at high transverse mass values. Events involving a hadronic decay of a τ-lepton originating from $W \longrightarrow \tau_{\mathrm{had}}\nu$ in one of the two branches and a leptonic W boson decay in the other branch ($\ell\nu\tau_{\mathrm{had}}\nu$), are the dominant decay mode in selections with high values of m_{T}. Due to the additional neutrino in such events, the $\ell\nu\tau_{\mathrm{had}}\nu$ decay mode does not exhibit the same kinematic endpoint as the semi-leptonic one. Finally, di-leptonic decays ($\ell\nu\ell\nu$) and events with a leptonically decaying τ-lepton ($\ell\nu\tau_{\ell}\nu$), where one of the two leptons is not reconstructed, play a sub-dominant but non-negligible role in all regions. Other $t\bar{t}$ decay modes are negligible in all analysis selections.

In the low-mass regions with moderate values in m_{T} not far above its kinematic endpoint, 80% (40%) of $t\bar{t}$ events involve the semi-leptonic decay mode in the control region (signal region). The sub-dominant decay mode in these regions involves the $\ell\nu\tau_{\mathrm{had}}\nu$ decay mode, with a contribution of 25% and 10% in TR-LM and SR-LM, respectively. Di-leptonic and $\ell\nu\tau_{\ell}\nu$ decay modes each contribute about 15% of all events in TR-LM and about 3% in SR-LM. Overall, the composition in the low-mass regions is hence not exactly the same in the control and signal regions, but the agreement is still considered to be acceptable. With about 45% (36%) and 30% (35%), the largest contributions in TR-MM (SR-MM) originate from $\ell\nu\tau_{\mathrm{had}}\nu$ decays and di-leptonic events, respectively. Events with a $\ell\nu\tau_{\ell}\nu$ decay contribute to about

10% (15%) in TR-MM (SR-MM). In the high-mass control and signal regions with a high requirement on m_{T}, the majority (about 50%) of events involve the $\ell\nu\tau_{\mathrm{had}}\nu$ decay mode, while the di-leptonic and $\ell\nu\tau_{\ell}\nu$ decay modes contribute with about 30% and 20%, respectively. Overall, the compositions of the different $t\bar{t}$ decay modes in each control region are thus similar to the contributions in the respective signal region, meaning that the proportions of $t\bar{t}$ processes constrained through the profie likelihood fit in the CRs are similar to those in the SRs to be estimated.

Signal contamination in the $t\bar{t}$ CRs is avoided by inverting the requirement on $m_{b\bar{b}}$, i.e. placing the $t\bar{t}$ CRs in the $m_{b\bar{b}}$ sideband. The maximum signal contamination over the entire signal grid is 0.8%, 1.1% and 1.9% for TR-LM, TR-MM and TR-HM, respectively, and thus negligible. Figures 6.3(a) to 6.3(c) show the signal contamination in the $t\bar{t}$ CRs over the full signal grid.

Control region for W + jets

Events from W + jets production present the second largest contribution of SM background processes in most SRs. A single W + jets control region, called WR in the following, is defined by replacing the signal region requirements on m_{T} and $m_{b\bar{b}}$ with $50\,\mathrm{GeV} < m_{\mathrm{T}} < 100\,\mathrm{GeV}$ and $50\,\mathrm{GeV} < m_{b\bar{b}} < 80\,\mathrm{GeV}$, respectively. No bins in m_{CT} or m_{T} are defined for WR, as the composition of W + jets is approximately constant in all regions.

Applying a low requirement on m_{T} allows to predominantly select events below the kinematic endpoint of the transverse mass of the W boson, resulting in a high statistics control region with a pre-fit W + jets purity of roughly 52.5%. The sub-dominant background component of WR is $t\bar{t}$ with 35.2%. Small contributions of 7.0% and 4.2% originate from single top and diboson processes, respectively. The composition of W + jets events in WR and all signal regions is found to be dominated by W boson production in association with two real b-jets. Minor contributions originate from processes with mis-tagged c-jets or light-flavour jets.

As was the case for the $t\bar{t}$ control regions, placing WR off the Higgs mass peak allows to achieve a tolerable maximum signal contamination of only 2.4% without affecting the composition of processes in the W + jets background too much. Most signal points have significantly less than 1% signal contamination in WR, as can be seen in fig. 6.3(d).

Control region for single top

Single top processes result in significant background contributions in some SRs, necessitating a proper semi-data-driven estimation. A single top control region (STR) is defined starting from the SRs by replacing the Higgs mass window cut on $m_{b\bar{b}}$ with $m_{b\bar{b}} > 195\,\mathrm{GeV}$ and removing the bins in m_{CT}.

The sideband approach achieves again a low maximum signal contamination of roughly 0.8%. The signal contamination across the entire signal grid is shown in fig. 6.3(e). The pre-fit purity of the single top processes in STR is 51.7% and sub-dominant contributions arise from $t\bar{t}$ processes (29%), W + jets (10%) and $t\bar{t}+V$ (6%) production.

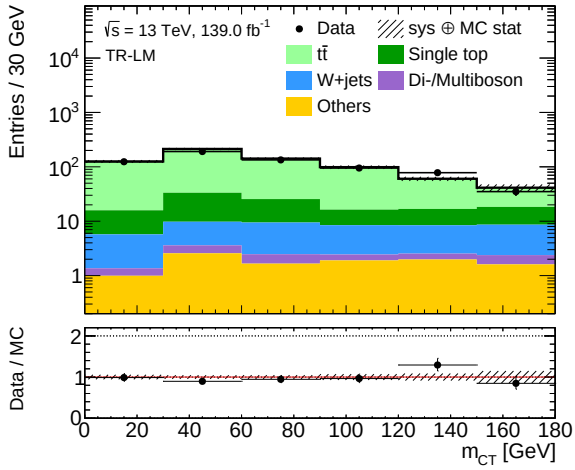

(a) TR-LM

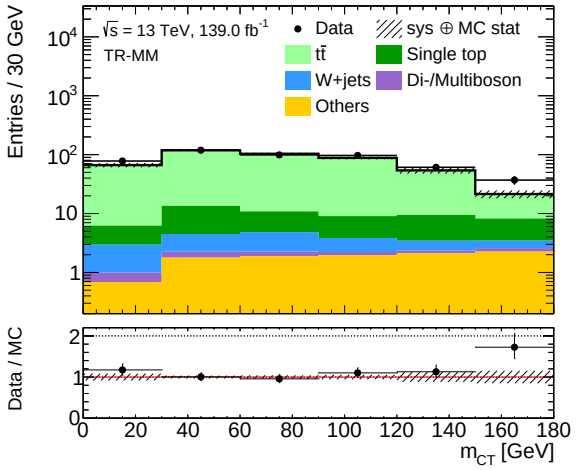

(b) TR-MM

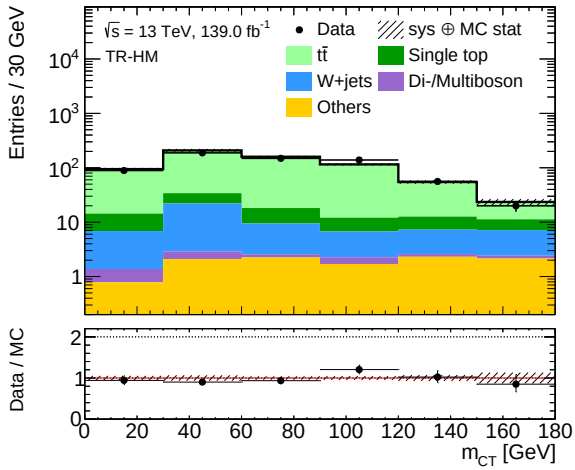

(c) TR-HM

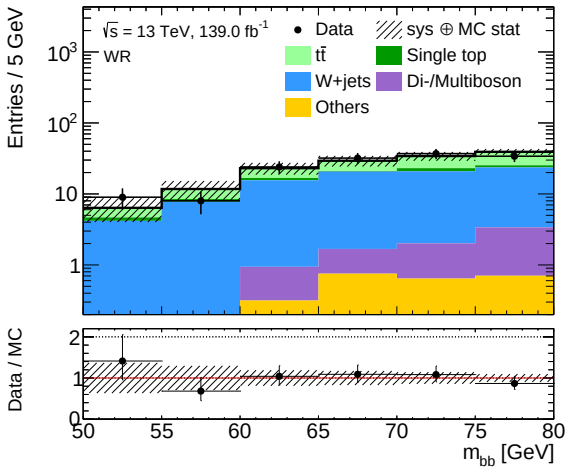

(d) WR

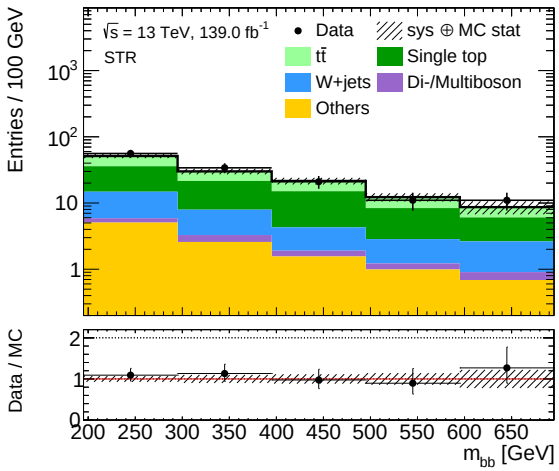

(e) STR

Figure 6.2: Exemplary pre-fit distributions for each control region. As laid out in the beginning of this chapter, the shaded region includes MC statistical uncertainty as well as experimental uncertainties, added in quadrature. The dominant backgrounds are normalised using the procedure described in section 6.1.3. A good agreement between MC expectation and data is observed in all CRs.

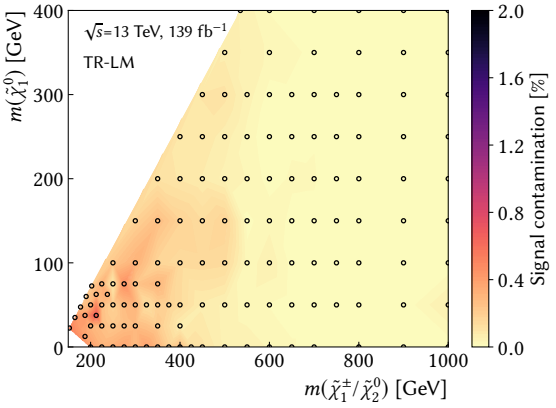

(a) TR-LM

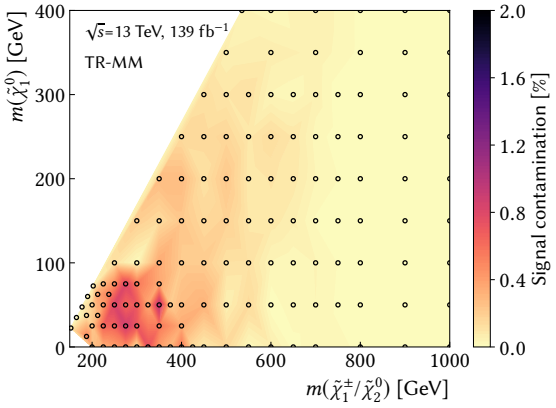

(b) TR-MM

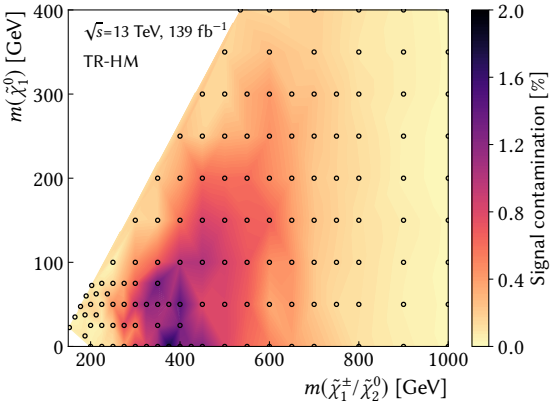

(c) TR-HM

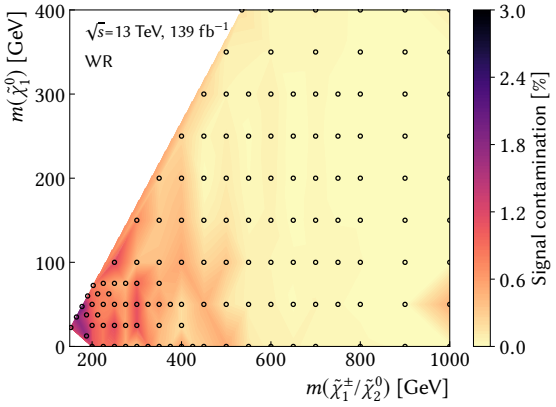

(d) WR

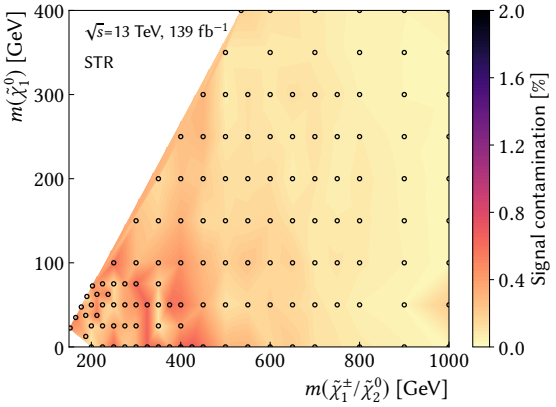

(e) STR

Figure 6.3: Signal contamination for all CRs throughout the signal grid. The space between the signal points (indicated by the black circles) is interpolated using Delaunay triangles.

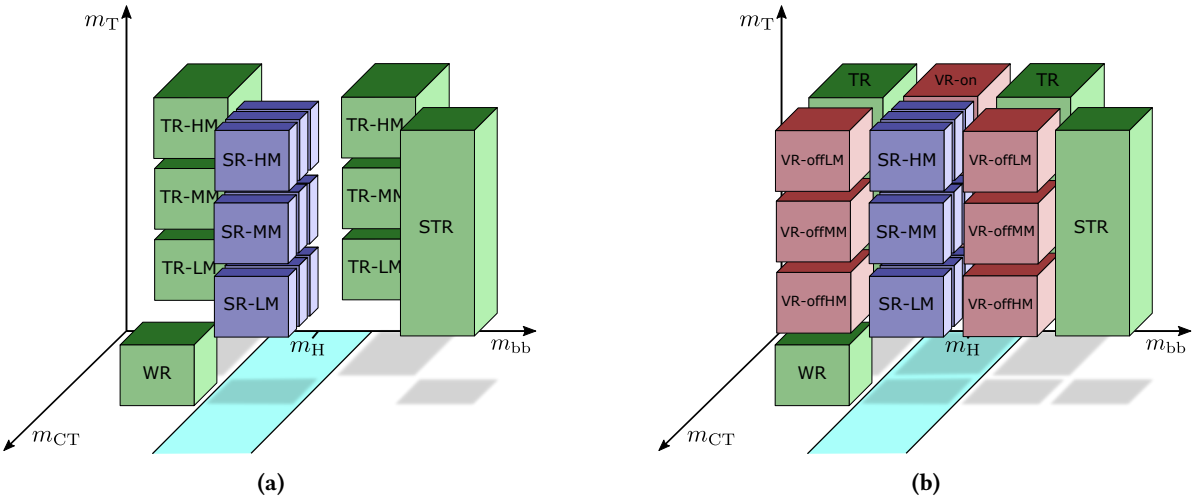

Figure 6.4: Configuration of (a) the CRs placed around the SRs off the $m_{b\bar{b}}$ window and (b) the validation regions in the phase space between the CRs and SRs. The VRs are arranged such that each of the extrapolations can be validated separately for SR-LM, SR-MM and SR-HM.

6.3 Validation regions

Two sets of VRs regions are introduced in order to verify the extrapolations over the different distributions. The selections defining all VRs are summarised in table 6.1. The first set, called VR-on is situated on the Higgs boson mass peak but with the m_{CT} requirement inverted to $m_{\mathrm{CT}} < 180\,\mathrm{GeV}$. This allows the VR-on regions to validate the extrapolation over $m_{b\bar{b}}$, performed when extrapolating the background estimate from the control regions into the signal regions. Three disjunct VR-on regions are introduced, with m_{T} requirements matching those of the SRs, such that the extrapolations can be validated separately for each signal region. The three VR-on regions are aptly named VR-onLM, VR-onMM and VR-onHM. A similar composition of $t\bar{t}$ decay modes as in the control and signal regions is observed in the VR-on regions, necessary for a trustworthy validation of the $t\bar{t}$ estimate. A maximum signal contamination of about 5%–14% is achieved, depending on the requirement in m_{T}. As can be seen from fig. A.10, most signal points have a signal contamination well below 5% for all VR-on regions.

The second set of VRs is located on both sides off the Higgs boson mass peak at same values in m_{CT} than the SRs. This set of *off-peak* VRs, called VR-off, is used to validate the extrapolation over the $m_{b\bar{b}}$ distribution performed in the case of STR. Additionally, the VR-off regions validate the extrapolation over the m_{CT} performed in the $t\bar{t}$ control regions. Similar to the on-peak validation regions, the VR-off regions are split into m_{T} bins matching the signal regions, allowing a validation of the background estimate in their respective signal region. The bins in VR-off are called VR-offLM, VR-offMM and VR-offHM. The maximum signal contamination in the VR-off regions is found to be about 7%–13%, depending on the requirement on m_{T}. Most signal points, however, reveal a signal contamination in the VR-off regions of less than 3% (cf. fig. A.10).

Part III

Reinterpretation

Part IV

Summary and Outlook

Part V

Appendices

Appendix A

Additional analysis material

This appendix provides additional analysis material for the 1ℓ search presented in part II of this thesis.

A.1 Kinematic distributions

Figure A.1 illustrates the dependence of the distributions of relevant kinematic observables on the electroweakino mass scale and the mass difference between $\tilde{\chi}_1^\pm/\tilde{\chi}_2^0$ and $\tilde{\chi}_1^0$. In the plots on the left column of fig. A.1, only $m(\tilde{\chi}_1^\pm/\tilde{\chi}_2^0)$ is varied while $m(\tilde{\chi}_1^0)$ is kept to be massless. On the right-hand side of fig. A.1, $m(\tilde{\chi}_1^\pm/\tilde{\chi}_2^0)$ is fixed at 450 GeV, while $m(\tilde{\chi}_1^0)$ is varied. As can be observed, model points with increasing $\tilde{\chi}_1^\pm/\tilde{\chi}_2^0$ mass show increasing values in kinematic observables like $E_\mathrm{T}^\mathrm{miss}$, m_T, m_CT and the p_T of the lepton. Model points with increasingly small electroweakino mass differences tend to exhibit less $E_\mathrm{T}^\mathrm{miss}$ and overall softer objects (as e.g. more events with leptons with relatively low p_T).

A.2 Signal region optimisation

A.2.1 Raw results from *N*-dimensional scan

Figure A.2 shows the results of the N-dimensional cut scan for all benchmark signal points considered. As in chapter 5, three different uncertainty configurations are used for computing the significance Z_B, and all values are computed for the two statistically independent subsets of the MC datasets used during the N-dimensional scan. This approach allows to gauge the impact of statistical fluctuations on the cut combinations tested.

By choosing a well-performing cut combination for each benchmark point, the optimised selections in figs. A.3 to A.8 are found after a round of $N-1$ plots. As discussed in section 5.2.2 the optimal cut combinations for each benchmark signal point are consolidated into multiple signal regions designed to be sensitive to different kinematic regions of the model parameter space.

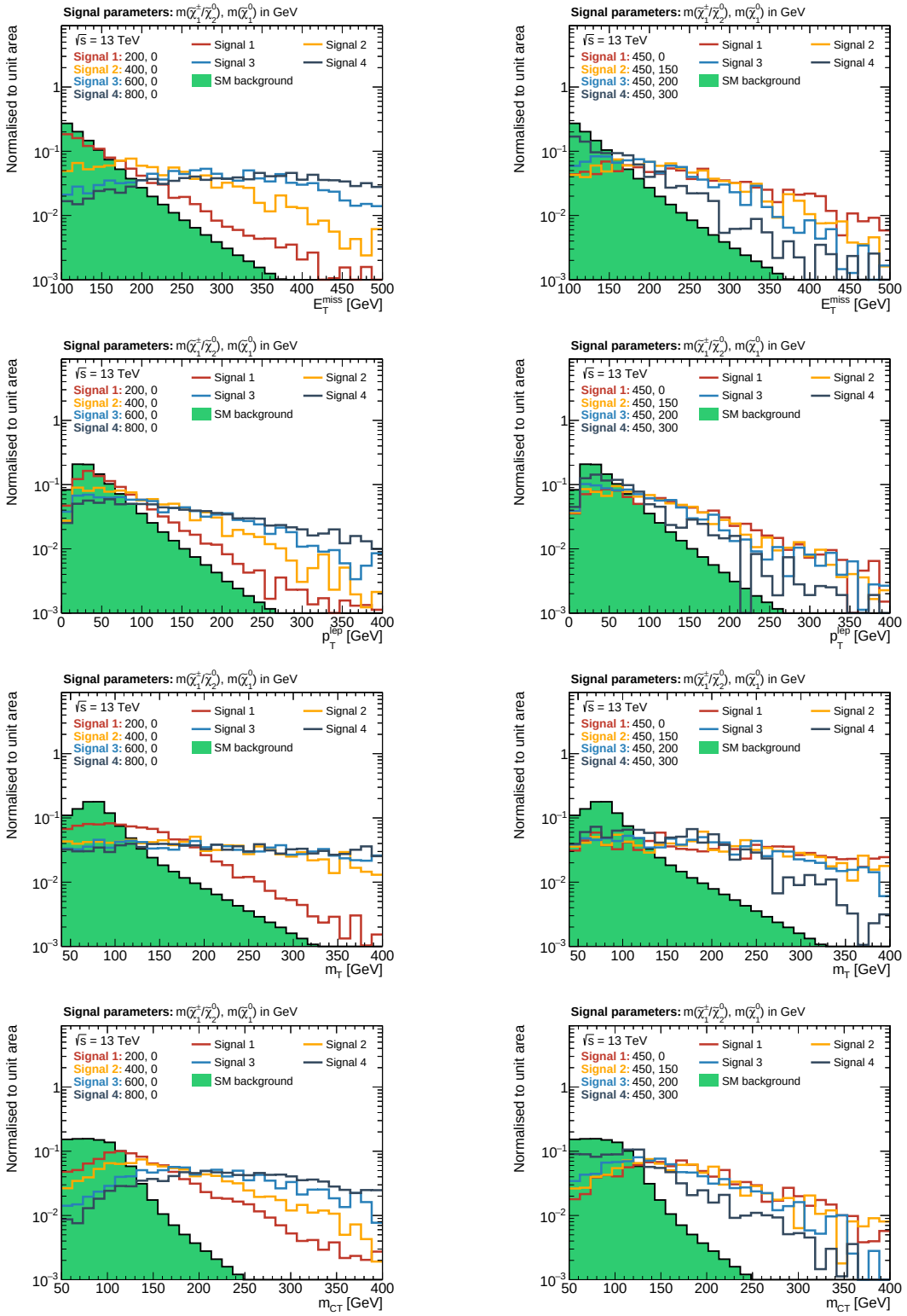

Figure A.1: Dependence of some of the kinematic observables on the $\tilde{\chi}_1^\pm/\tilde{\chi}_2^0$ mass scale (left) and $\tilde{\chi}_1^\pm/\tilde{\chi}_2^0-\tilde{\chi}_1^0$ mass differences (right). The simulated SM backgrounds are stacked on top of each other and summarised in a single 'SM' histogram. Distributions from exemplary signal models with the quoted mass parameters are overlaid. In order to emphasise the shape differences, both total background and signal distributions are normalised to unity. A preselection requiring a lepton, at least two jets and $E_{\mathrm{T}}^{\mathrm{miss}} > 100\,\mathrm{GeV}$ is applied.

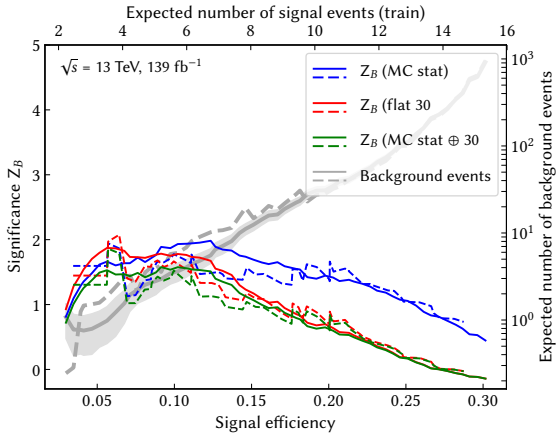

(a) $m(\tilde{\chi}_1^\pm/\tilde{\chi}_2^0), m(\tilde{\chi}_1^0) = 800, 250$ GeV

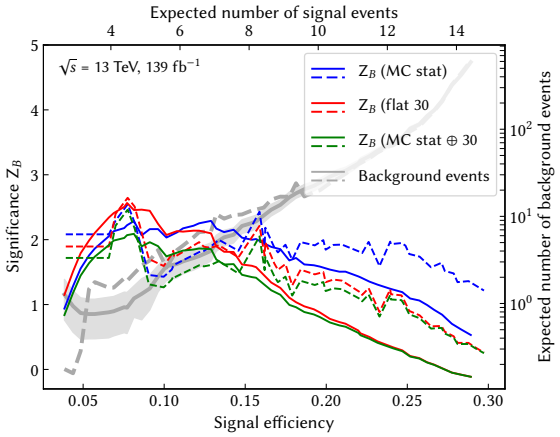

(b) $m(\tilde{\chi}_1^\pm/\tilde{\chi}_2^0), m(\tilde{\chi}_1^0) = 800, 150$ GeV

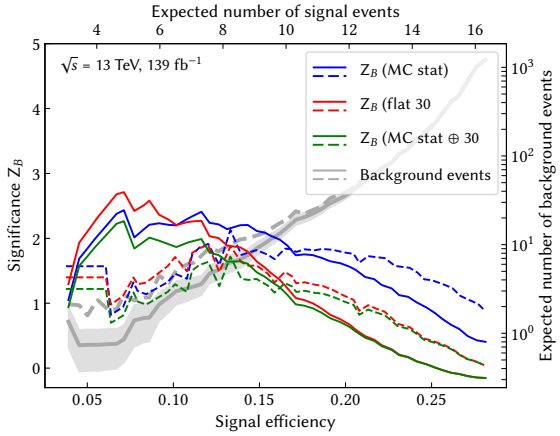

(c) $m(\tilde{\chi}_1^\pm/\tilde{\chi}_2^0), m(\tilde{\chi}_1^0) = 800, 0$ GeV

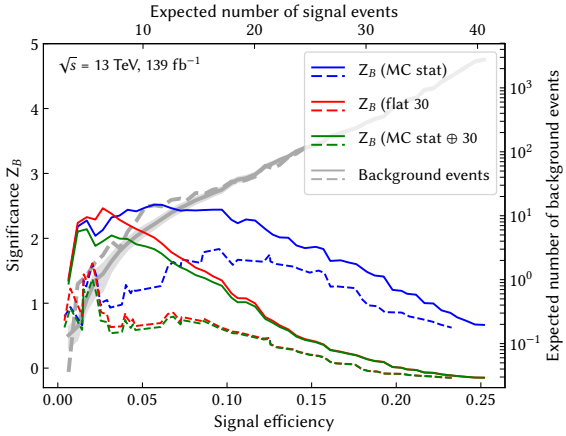

(d) $m(\tilde{\chi}_1^\pm/\tilde{\chi}_2^0), m(\tilde{\chi}_1^0) = 600, 300$ GeV

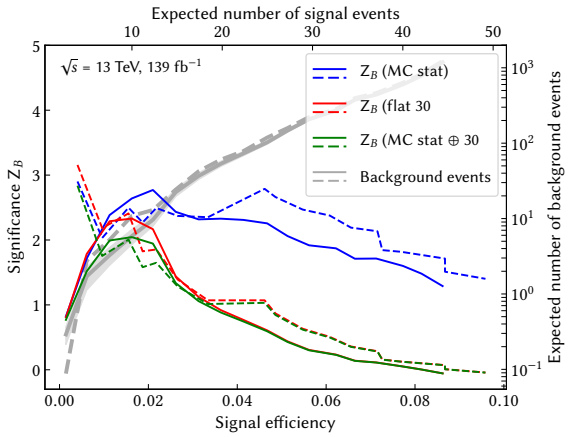

(e) $m(\tilde{\chi}_1^\pm/\tilde{\chi}_2^0), m(\tilde{\chi}_1^0) = 400, 200$ GeV

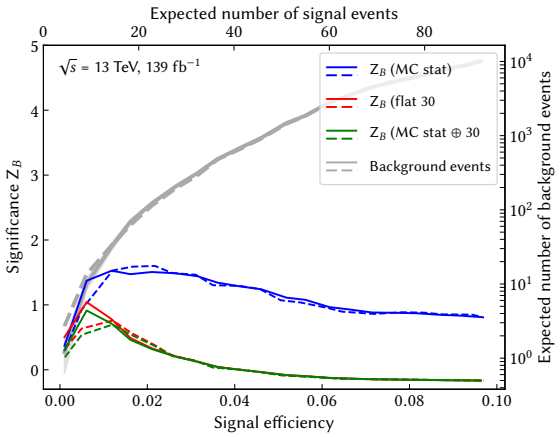

(f) $m(\tilde{\chi}_1^\pm/\tilde{\chi}_2^0), m(\tilde{\chi}_1^0) = 300, 150$ GeV

Figure A.2: Results of the N-dimensional cut scan for all benchmark points. The binomial discovery significance Z_B is plotted against the signal efficiency for varying uncertainty configurations. Additionally, the expected SM background rates are shown, including statistical uncertainties for one of the two statistically independent samples (shaded area). The solid and dashed lines represent the two statistically independent subsets that the MC datasets are split into.

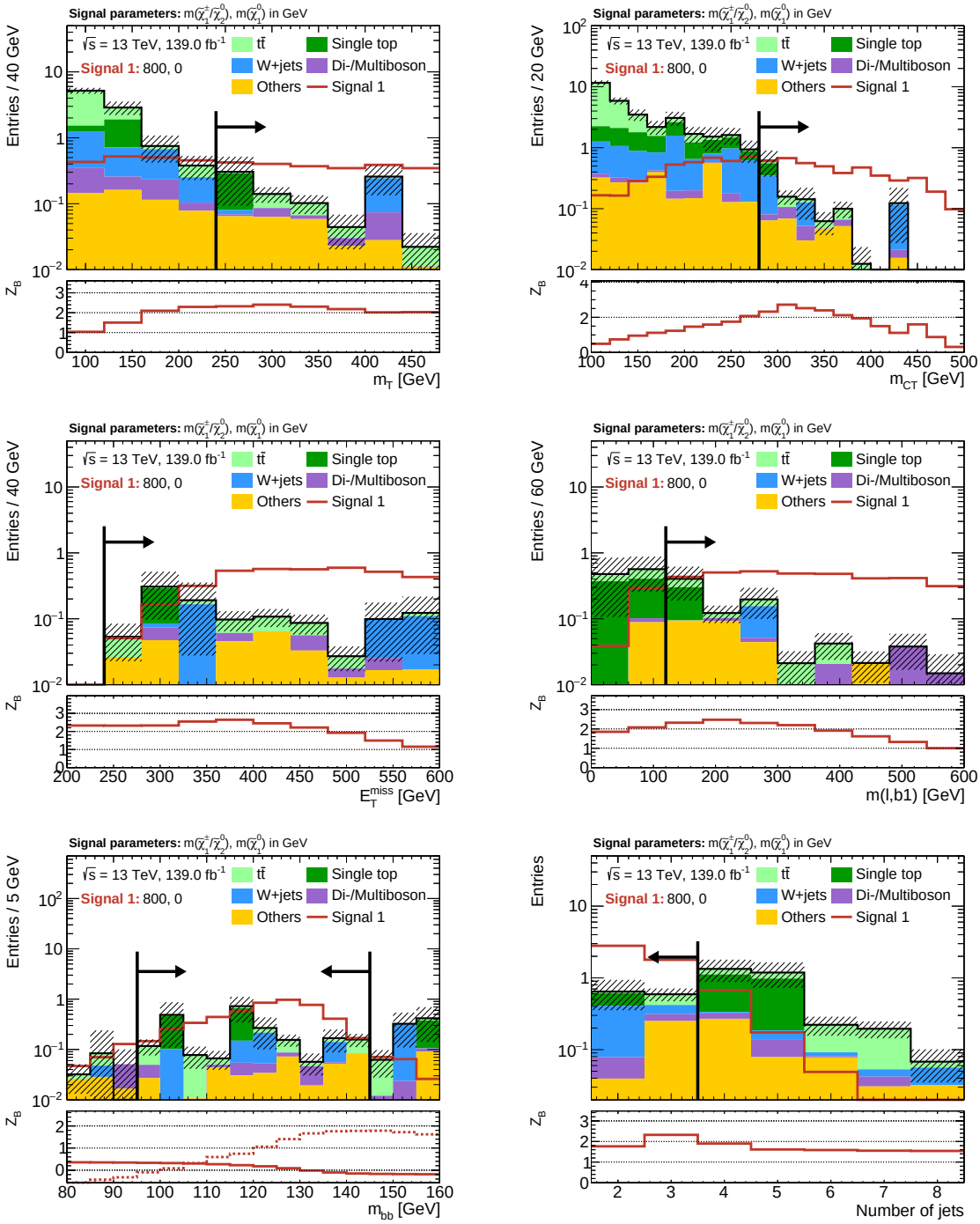

Figure A.3: $N-1$ plots for the chosen cut combination for the $(m(\tilde{\chi}_1^\pm/\tilde{\chi}_2^0), m(\tilde{\chi}_1^0)) = (800\,\text{GeV}, 0\,\text{GeV})$ signal point. The shaded region includes MC statistical as well as 30% systematic uncertainties (added in quadrature) on the background. The significance is computed using the binomial discovery significance using the uncertainty on the background.

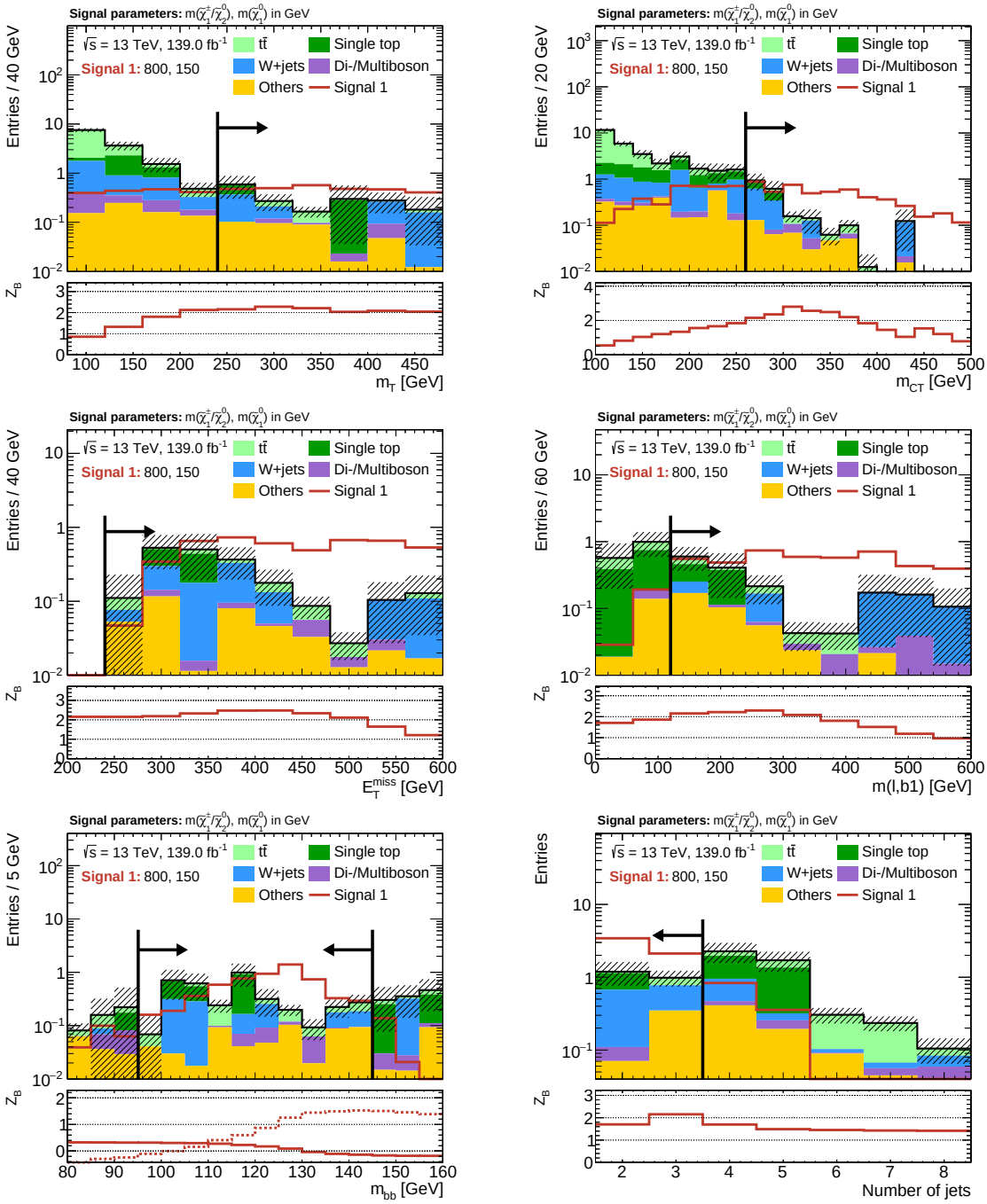

Figure A.4: N-1 plots for the chosen cut combination for the $(m(\tilde{\chi}_1^\pm/\tilde{\chi}_2^0), m(\tilde{\chi}_1^0)) = (800\,\text{GeV}, 150\,\text{GeV})$ signal point. The shaded region includes MC statistical as well as 30% systematic uncertainties (added in quadrature) on the background. The significance is computed using the binomial discovery significance using the uncertainty on the background.

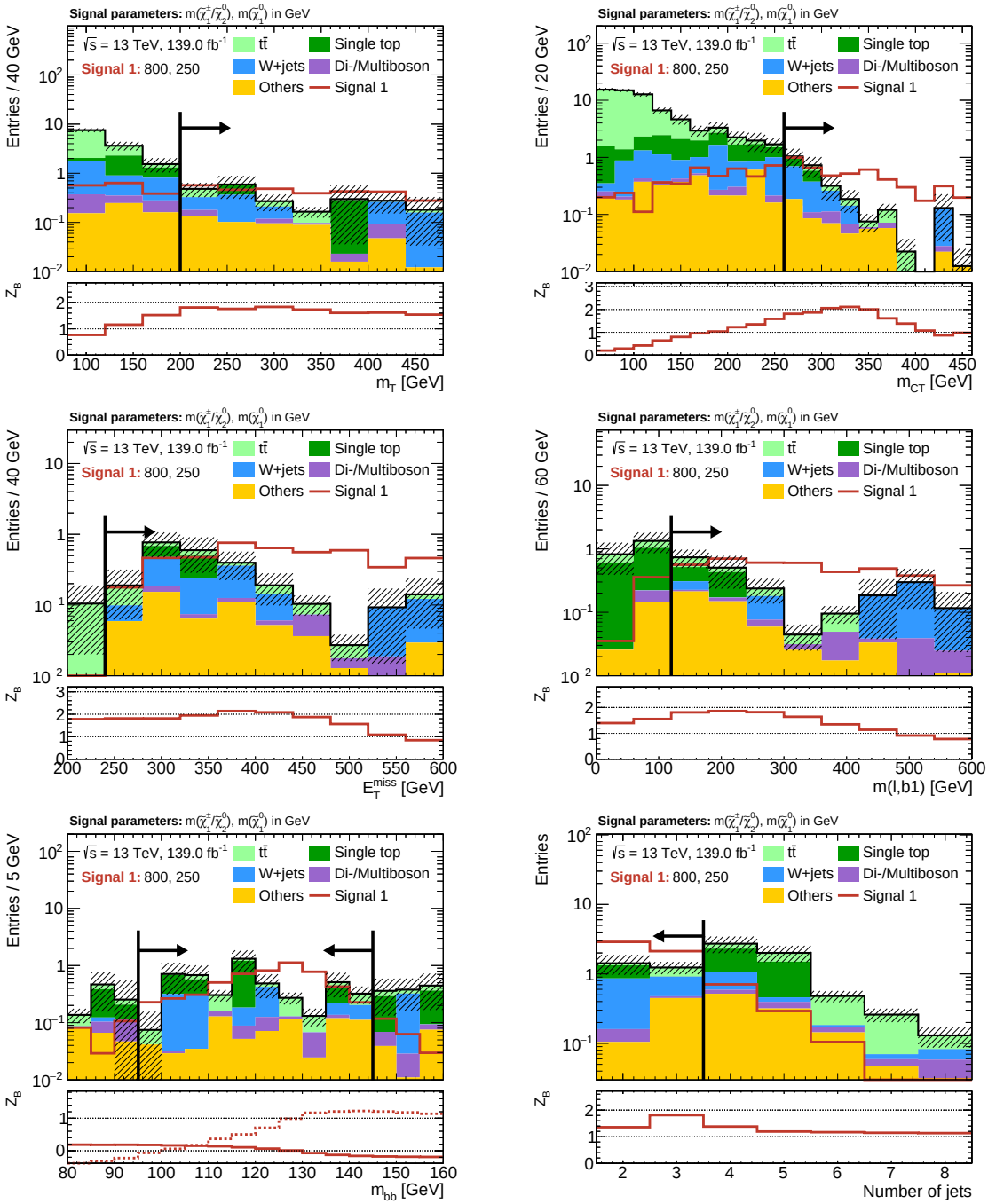

Figure A.5: $N-1$ plots for the chosen cut combination for the $(m(\tilde{\chi}_1^\pm/\tilde{\chi}_2^0), m(\tilde{\chi}_1^0)) = (800\,\text{GeV}, 250\,\text{GeV})$ signal point. The shaded region includes MC statistical as well as 30% systematic uncertainties (added in quadrature) on the background. The significance is computed using the binomial discovery significance using the uncertainty on the background.

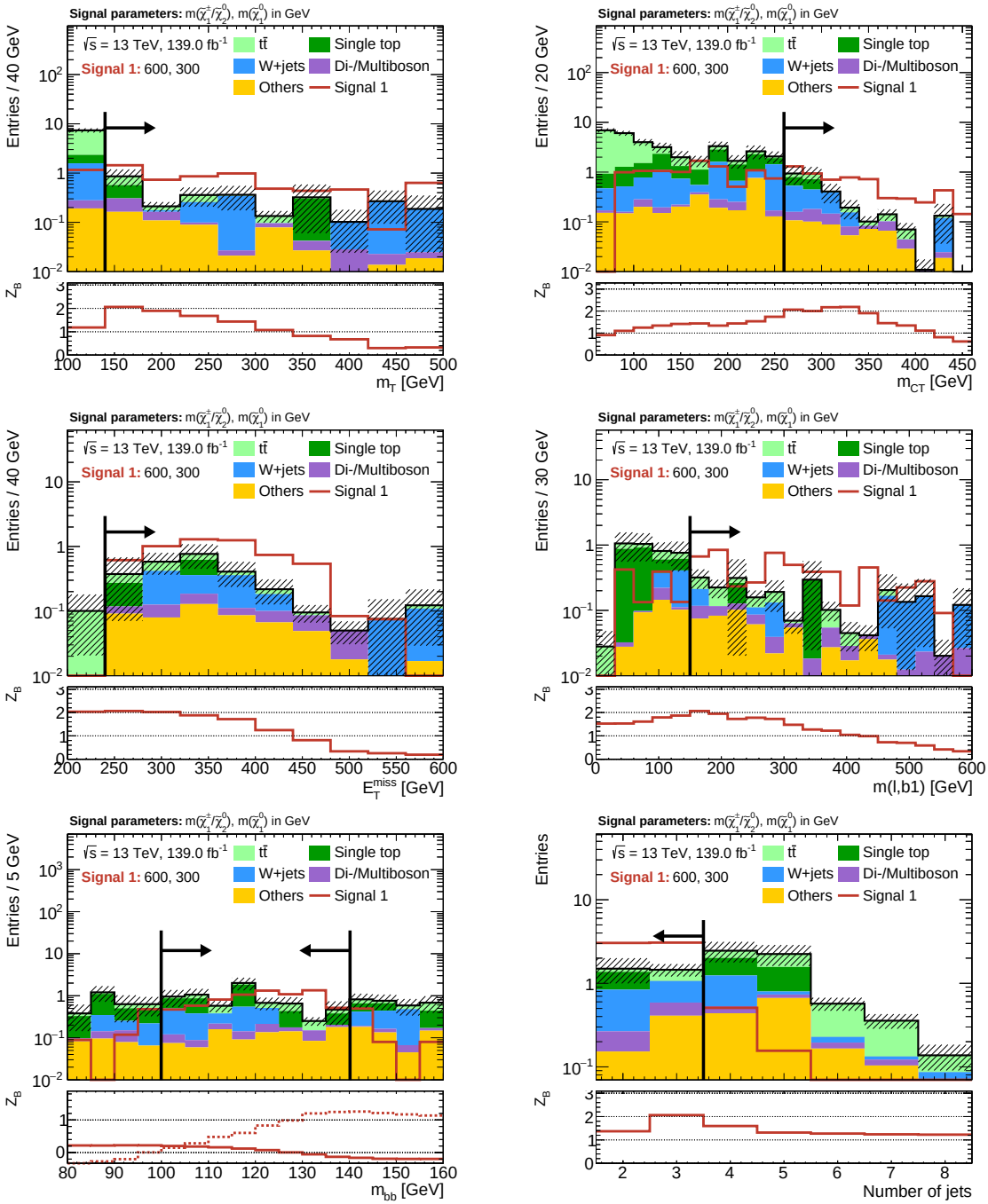

Figure A.6: $N-1$ plots for the chosen cut combination for the $(m(\tilde{\chi}_1^\pm/\tilde{\chi}_2^0), m(\tilde{\chi}_1^0)) = (600\,\text{GeV}, 300\,\text{GeV})$ signal point. The shaded region includes MC statistical as well as 30% systematic uncertainties (added in quadrature) on the background. The significance is computed using the binomial discovery significance using the uncertainty on the background.

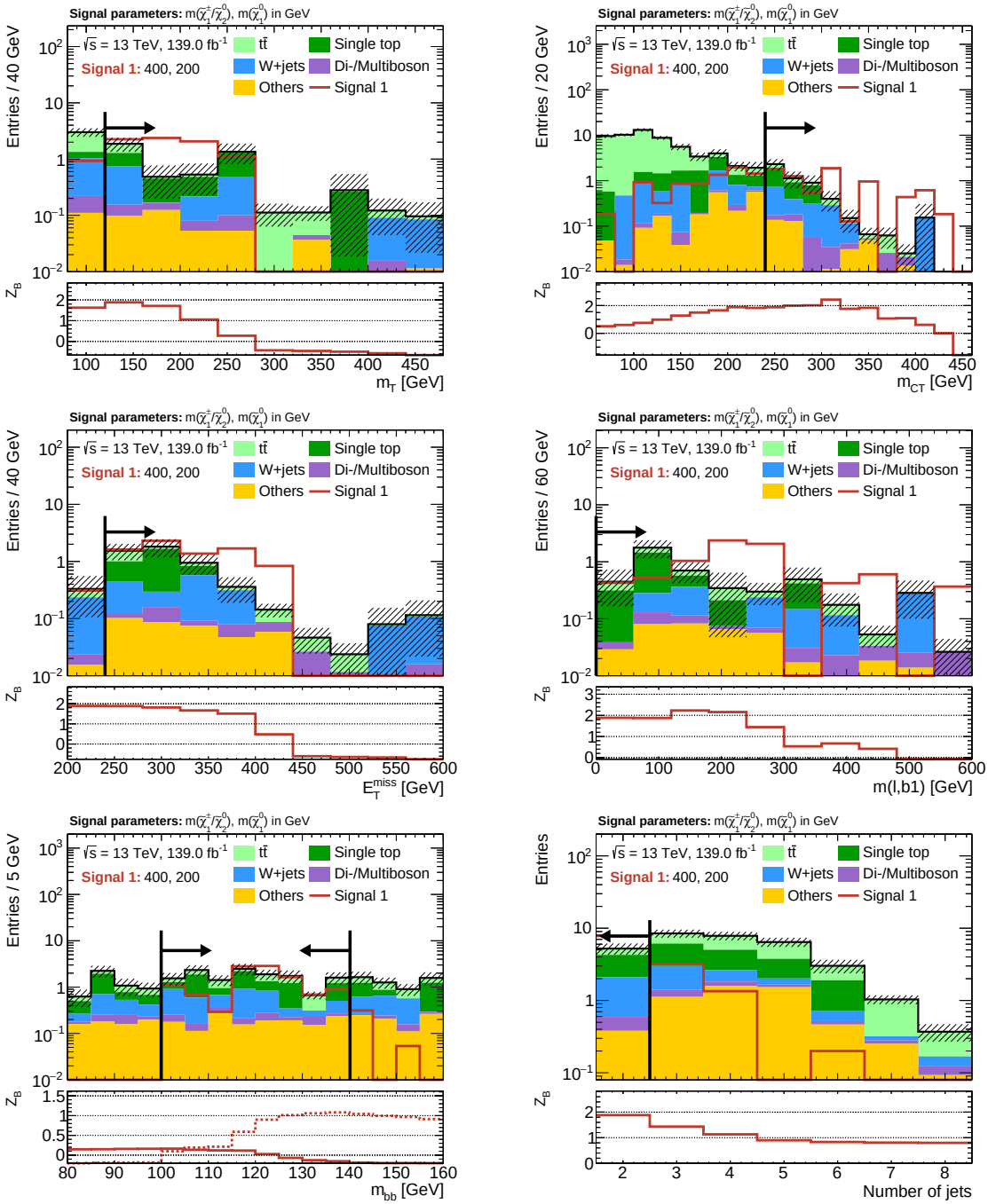

Figure A.7: N-1 plots for the chosen cut combination for the $(m(\tilde{\chi}_1^\pm/\tilde{\chi}_2^0), m(\tilde{\chi}_1^0)) = (400\,\text{GeV}, 200\,\text{GeV})$ signal point. The shaded region includes MC statistical as well as 30% systematic uncertainties (added in quadrature) on the background. The significance is computed using the binomial discovery significance using the uncertainty on the background.

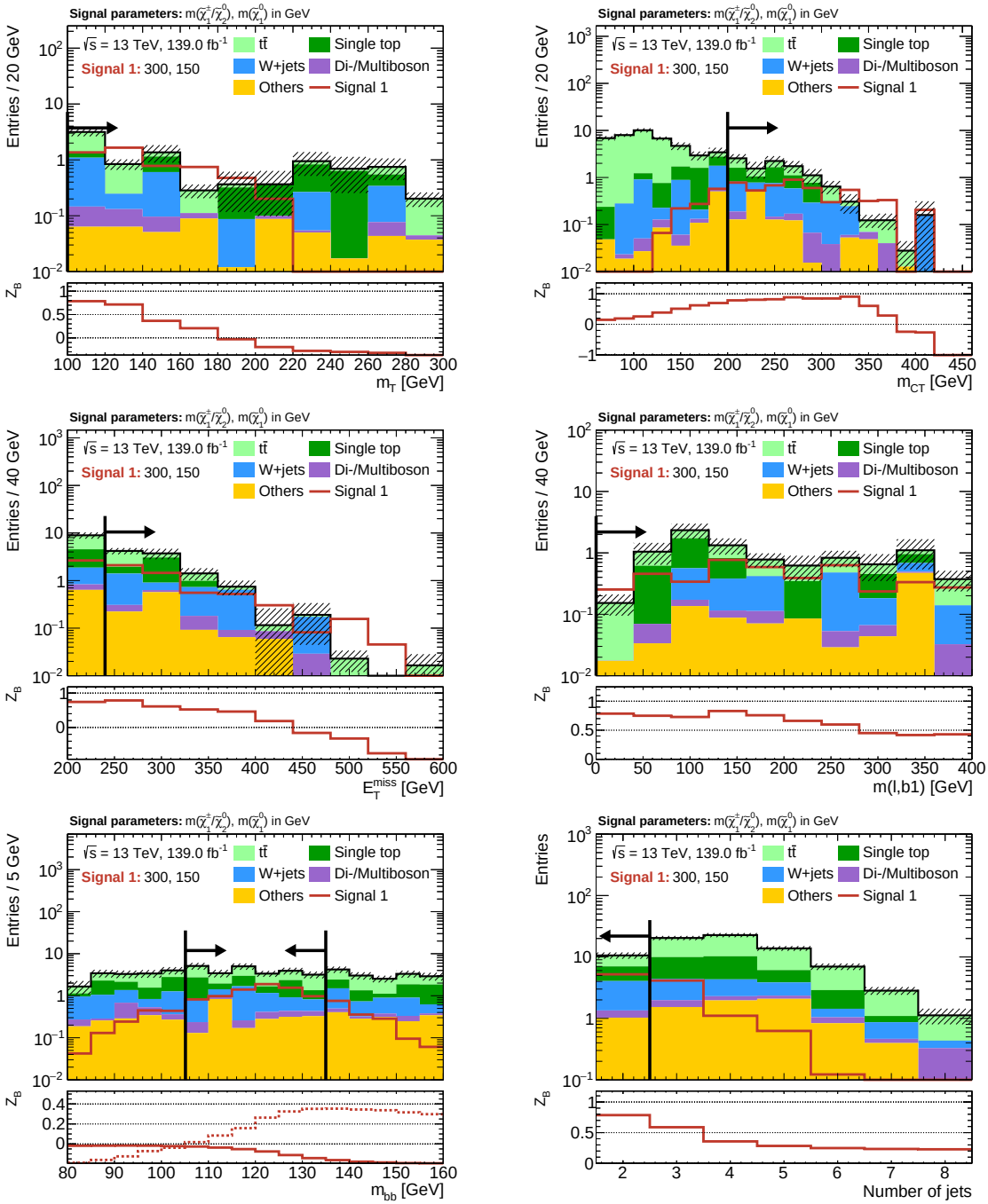

Figure A.8: $N-1$ plots for the chosen cut combination for the $(m(\tilde{\chi}_1^\pm/\tilde{\chi}_2^0), m(\tilde{\chi}_1^0)) = (300\,\text{GeV}, 150\,\text{GeV})$ signal point. The shaded region includes MC statistical as well as 30% systematic uncertainties (added in quadrature) on the background. The significance is computed using the binomial discovery significance using the uncertainty on the background.

A.2.2 Impact of $m_{\ell b_1}$1

As discussed in section 4.6, the distribution of $m_{\ell b_1}$ has a kinematic endpoint at about 153 GeV for $t\bar{t}$ and single top production events where the lepton and leading b-jet originate from the same top quark decay. In the SUSY processes considered, $m_{\ell b_1}$ depends on the mass-scale of the electroweakinos pair-produced, and thus offers especially good discriminative power in the high electroweakino mass regime targeted by SR-HM.

Figure A.9 illustrates the impact of adding a requirement of $m_{\ell b_1} > 120$ GeV in SR-HM, revealing a noticeable increase in sensitivity towards high electroweakino masses. Studies have shown that the addition of $m_{\ell b_1} > 120$ GeV to the remaining signal regions does not improve the sensitivity further.

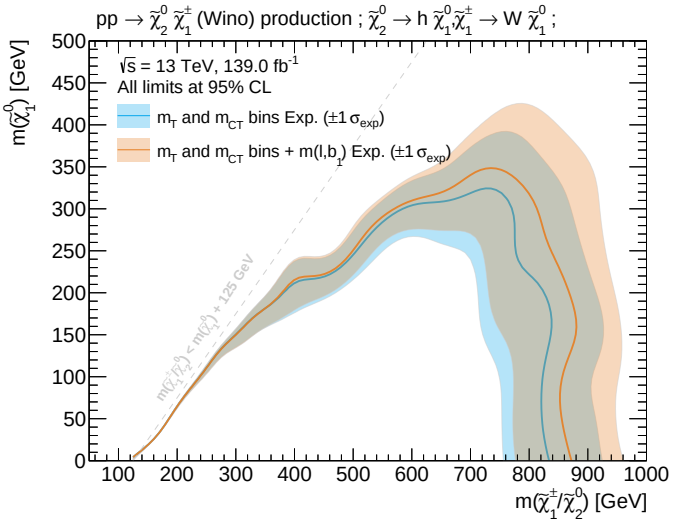

Figure A.9: Comparison of different shape-fit configurations, illustrating the sensitivity increase achieved through a requirement on high $m_{\ell b_1}$ values in SR-HM on top of the two-dimensional shape-fit in m_{T} and m_{CT}. All exclusion limits shown are expected limits at 95% CL, using MC statistical and 30% systematic uncertainties. Background estimation in the signal regions is taken directly from MC for all SM backgrounds.

A.3 Background estimation

The signal contamination in all validation regions is shown in fig. A.10. In the VR-off regions the maximum signal contamination is found to be about 7%–13%, depending on the requirement on m_{T}. In the VR-on regions, the maximum signal contamination amounts to about 5%–14%, depending again on the m_{T}-bin.

Figure A.11 provides a comprehensive summary of current results of ATLAS searches for SUSY. The limits on the sparticle masses set by different searches in various models and signatures are given.

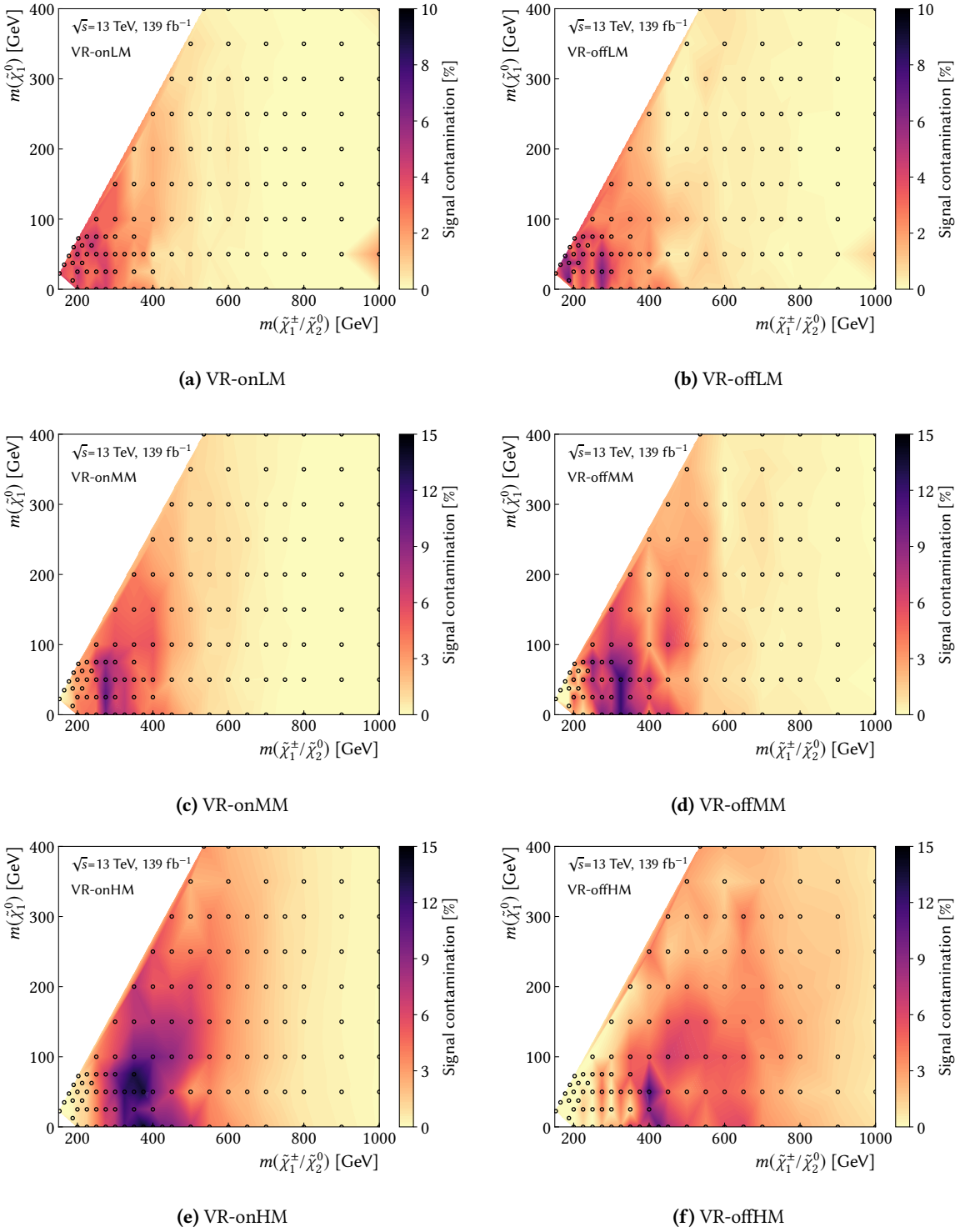

(a) VR-onLM **(b)** VR-offLM

(c) VR-onMM **(d)** VR-offMM

(e) VR-onHM **(f)** VR-offHM

Figure A.10: Signal contamination (shown on the *z-axis*) for all VRs throughout the signal grid. The space between the signal points (indicated by the black circles) is interpolated using Delaunay triangles.

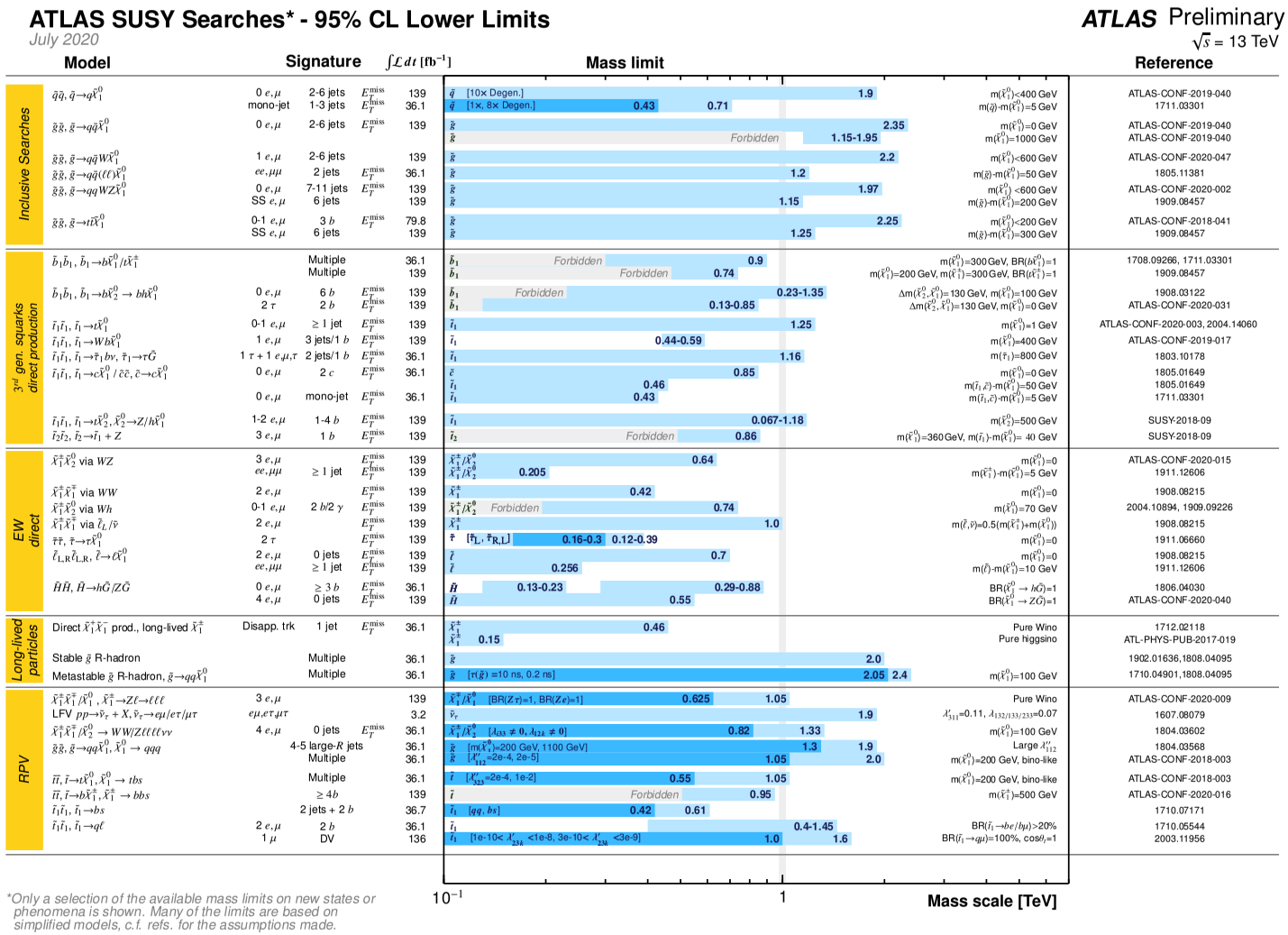

Figure A.11: Summary of the results of ATLAS searches for SUSY. A representative selection of the available search results is shown. Results are given with respect to the nominal cross section. In some cases additional dependencies are indicated by darker bands showing different model parameters. Figure adapted from Ref. [258].

Abbreviations

CR control region. 99–106

MC Monte Carlo. 99–102, 104, 179, 181–188

SM Standard Model. 99, 102, 103, 180, 181, 188

SR signal region. 99–103, 106

SUSY Supersymmetry. 99, 100, 188, 190

VR validation region. 100–102, 106, 189

Bibliography

[1] ATLAS Collaboration, "Observation of a new particle in the search for the Standard Model Higgs boson with the ATLAS detector at the LHC," *Phys. Lett. B* **716** (2012) 1, arXiv:1207.7214 [hep-ex].

[2] CMS Collaboration, "Observation of a new boson at a mass of 125 GeV with the CMS experiment at the LHC," *Phys. Lett. B* **716** (2012) 30, arXiv:1207.7235 [hep-ex].

[3] I. C. Brock and T. Schorner-Sadenius, *Physics at the terascale*. Wiley, Weinheim, 2011. https://cds.cern.ch/record/1354959.

[4] M. E. Peskin and D. V. Schroeder, *An Introduction to quantum field theory*. Addison-Wesley, Reading, USA, 1995. http://www.slac.stanford.edu/~mpeskin/QFT.html.

[5] S. P. Martin, "A Supersymmetry primer," arXiv:hep-ph/9709356v7 [hep-ph]. [Adv. Ser. Direct. High Energy Phys.18,1(1998)].

[6] M. Bustamante, L. Cieri, and J. Ellis, "Beyond the Standard Model for Montaneros," in *5th CERN - Latin American School of High-Energy Physics*. 11, 2009. arXiv:0911.4409 [hep-ph].

[7] L. Brown, *The Birth of particle physics*. Cambridge University Press, Cambridge Cambridgeshire New York, 1986.

[8] P. J. Mohr, D. B. Newell, and B. N. Taylor, "CODATA Recommended Values of the Fundamental Physical Constants: 2014," *Rev. Mod. Phys.* **88** no. 3, (2016) 035009, arXiv:1507.07956 [physics.atom-ph].

[9] Particle Data Group, "Review of Particle Physics," *Progress of Theoretical and Experimental Physics* **2020** no. 8, (08, 2020) , https://academic.oup.com/ptep/article-pdf/2020/8/083C01/34673722/ptaa104.pdf. https://doi.org/10.1093/ptep/ptaa104. 083C01.

[10] Super-Kamiokande Collaboration, "Evidence for oscillation of atmospheric neutrinos," *Phys. Rev. Lett.* **81** (1998) 1562–1567, arXiv:hep-ex/9807003 [hep-ex].

[11] Z. Maki, M. Nakagawa, and S. Sakata, "Remarks on the unified model of elementary particles," *Prog. Theor. Phys.* **28** (1962) 870–880. [,34(1962)].

[12] N. Cabibbo, "Unitary symmetry and leptonic decays," *Phys. Rev. Lett.* **10** (Jun, 1963) 531–533. https://link.aps.org/doi/10.1103/PhysRevLett.10.531.

[13] M. Kobayashi and T. Maskawa, "CP Violation in the Renormalizable Theory of Weak Interaction," *Prog. Theor. Phys.* **49** (1973) 652–657.

[14] E. Noether and M. A. Tavel, "Invariant variation problems," arXiv:physics/0503066.

[15] J. C. Ward, "An identity in quantum electrodynamics," *Phys. Rev.* **78** (Apr, 1950) 182–182. https://link.aps.org/doi/10.1103/PhysRev.78.182.

[16] Y. Takahashi, "On the generalized ward identity," *Il Nuovo Cimento (1955-1965)* **6** no. 2, (Aug, 1957) 371–375. https://doi.org/10.1007/BF02832514.

[17] G. 'tHooft, "Renormalization of massless yang-mills fields," *Nuclear Physics B* **33** no. 1, (1971) 173 – 199. http://www.sciencedirect.com/science/article/pii/0550321371903956.

[18] J. Taylor, "Ward identities and charge renormalization of the yang-mills field," *Nuclear Physics B* **33** no. 2, (1971) 436 – 444. http://www.sciencedirect.com/science/article/pii/0550321371902975.

[19] A. A. Slavnov, "Ward identities in gauge theories," *Theoretical and Mathematical Physics* **10** no. 2, (Feb, 1972) 99–104. https://doi.org/10.1007/BF01090719.

[20] C. N. Yang and R. L. Mills, "Conservation of isotopic spin and isotopic gauge invariance," *Phys. Rev.* **96** (Oct, 1954) 191–195. https://link.aps.org/doi/10.1103/PhysRev.96.191.

[21] K. G. Wilson, "Confinement of quarks," *Phys. Rev. D* **10** (Oct, 1974) 2445–2459. https://link.aps.org/doi/10.1103/PhysRevD.10.2445.

[22] T. DeGrand and C. DeTar, *Lattice Methods for Quantum Chromodynamics*. World Scientific, Singapore, 2006. https://cds.cern.ch/record/1055545.

[23] S. L. Glashow, "Partial-symmetries of weak interactions," *Nuclear Physics* **22** no. 4, (1961) 579 – 588. http://www.sciencedirect.com/science/article/pii/0029558261904692.

[24] S. Weinberg, "A model of leptons," *Phys. Rev. Lett.* **19** (Nov, 1967) 1264–1266. https://link.aps.org/doi/10.1103/PhysRevLett.19.1264.

[25] A. Salam and J. C. Ward, "Weak and electromagnetic interactions," *Il Nuovo Cimento (1955-1965)* **11** no. 4, (Feb, 1959) 568–577. https://doi.org/10.1007/BF02726525.

[26] C. S. Wu, E. Ambler, R. W. Hayward, *et al.*, "Experimental test of parity conservation in beta decay," *Phys. Rev.* **105** (Feb, 1957) 1413–1415. https://link.aps.org/doi/10.1103/PhysRev.105.1413.

[27] M. Gell-Mann, "The interpretation of the new particles as displaced charge multiplets," *Il Nuovo Cimento (1955-1965)* **4** no. 2, (Apr, 1956) 848–866. https://doi.org/10.1007/BF02748000.

[28] K. Nishijima, "Charge Independence Theory of V Particles*," *Progress of Theoretical Physics* **13** no. 3, (03, 1955) 285–304, https://academic.oup.com/ptp/article-pdf/13/3/285/5425869/13-3-285.pdf. https://doi.org/10.1143/PTP.13.285.

[29] T. Nakano and K. Nishijima, "Charge Independence for V-particles*," *Progress of Theoretical Physics* **10** no. 5, (11, 1953) 581–582, https://academic.oup.com/ptp/article-pdf/10/5/581/5364926/10-5-581.pdf. https://doi.org/10.1143/PTP.10.581.

[30] F. Englert and R. Brout, "Broken symmetry and the mass of gauge vector mesons," *Phys. Rev. Lett.* **13** (Aug, 1964) 321–323. https://link.aps.org/doi/10.1103/PhysRevLett.13.321.

[31] P. W. Higgs, "Broken symmetries and the masses of gauge bosons," *Phys. Rev. Lett.* **13** (Oct, 1964) 508–509. https://link.aps.org/doi/10.1103/PhysRevLett.13.508.

[32] P. W. Higgs, "Spontaneous symmetry breakdown without massless bosons," *Phys. Rev.* **145** (May, 1966) 1156–1163. https://link.aps.org/doi/10.1103/PhysRev.145.1156.

[33] Y. Nambu, "Quasiparticles and Gauge Invariance in the Theory of Superconductivity," *Phys. Rev.* **117** (1960) 648–663. [,132(1960)].

[34] J. Goldstone, "Field Theories with Superconductor Solutions," *Nuovo Cim.* **19** (1961) 154–164.

[35] V. Brdar, A. J. Helmboldt, S. Iwamoto, and K. Schmitz, "Type-I Seesaw as the Common Origin of Neutrino Mass, Baryon Asymmetry, and the Electroweak Scale," *Phys. Rev. D* **100** (2019) 075029, arXiv:1905.12634 [hep-ph].

[36] G. 't Hooft and M. Veltman, "Regularization and renormalization of gauge fields," *Nuclear Physics B* **44** no. 1, (1972) 189 – 213. http://www.sciencedirect.com/science/article/pii/0550321372902799.

[37] G. L. Kane, *The supersymmetric world : the beginnings of the theory.* World Scientific, Singapore River Edge, N.J, 2000.

[38] F. Zwicky, "Die Rotverschiebung von extragalaktischen Nebeln," *Helv. Phys. Acta* **6** (1933) 110–127. https://cds.cern.ch/record/437297.

[39] V. C. Rubin and W. K. Ford, Jr., "Rotation of the Andromeda Nebula from a Spectroscopic Survey of Emission Regions," *Astrophys. J.* **159** (1970) 379–403.

[40] G. Bertone, D. Hooper, and J. Silk, "Particle dark matter: Evidence, candidates and constraints," *Phys. Rept.* **405** (2005) 279–390, arXiv:hep-ph/0404175.

[41] D. Clowe, M. Bradac, A. H. Gonzalez, *et al.*, "A direct empirical proof of the existence of dark matter," *Astrophys. J.* **648** (2006) L109–L113, arXiv:astro-ph/0608407 [astro-ph].

[42] A. Taylor, S. Dye, T. J. Broadhurst, *et al.*, "Gravitational lens magnification and the mass of abell 1689," *Astrophys. J.* **501** (1998) 539, arXiv:astro-ph/9801158.

[43] C. Bennett *et al.*, "Four year COBE DMR cosmic microwave background observations: Maps and basic results," *Astrophys. J. Lett.* **464** (1996) L1–L4, arXiv:astro-ph/9601067.

[44] G. F. Smoot *et al.*, "Structure in the COBE Differential Microwave Radiometer First-Year Maps," *ApJS* **396** (September, 1992) L1.

[45] WMAP Collaboration, "Nine-year Wilkinson Microwave Anisotropy Probe (WMAP) Observations: Final Maps and Results," *ApJS* **208** no. 2, (October, 2013) 20, arXiv:1212.5225 [astro-ph.CO].

[46] WMAP Collaboration, "Nine-year Wilkinson Microwave Anisotropy Probe (WMAP) Observations: Cosmological Parameter Results," *ApJS* **208** no. 2, (October, 2013) 19, arXiv:1212.5226 [astro-ph.CO].

[47] Planck Collaboration, "Planck 2018 results. I. Overview and the cosmological legacy of Planck," *Astron. Astrophys.* **641** (2020) A1, arXiv:1807.06205 [astro-ph.CO].

[48] A. Liddle, *An introduction to modern cosmology; 3rd ed.* Wiley, Chichester, Mar, 2015. https://cds.cern.ch/record/1976476.

[49] Planck Collaboration, "Planck 2018 results. VI. Cosmological parameters," *Astron. Astrophys.* **641** (2020) A6, arXiv:1807.06209 [astro-ph.CO].

[50] H. Georgi and S. L. Glashow, "Unity of all elementary-particle forces," *Phys. Rev. Lett.* **32** (Feb, 1974) 438–441. https://link.aps.org/doi/10.1103/PhysRevLett.32.438.

[51] I. Aitchison, *Supersymmetry in Particle Physics. An Elementary Introduction.* Cambridge University Press, Cambridge, 2007.

[52] Muon g-2 Collaboration, "Final Report of the Muon E821 Anomalous Magnetic Moment Measurement at BNL," *Phys. Rev. D* **73** (2006) 072003, arXiv:hep-ex/0602035.

[53] H. Baer and X. Tata, *Weak Scale Supersymmetry: From Superfields to Scattering Events.* Cambridge University Press, 2006.

[54] T. Aoyama *et al.*, "The anomalous magnetic moment of the muon in the Standard Model," *Phys. Rept.* **887** (2020) 1–166, arXiv:2006.04822 [hep-ph].

[55] Muon g-2 Collaboration, "Measurement of the Positive Muon Anomalous Magnetic Moment to 0.46 ppm," *Phys. Rev. Lett.* **126** no. 14, (2021) 141801, arXiv:2104.03281 [hep-ex].

[56] A. Czarnecki and W. J. Marciano, "The Muon anomalous magnetic moment: A Harbinger for 'new physics'," *Phys. Rev. D* **64** (2001) 013014, arXiv:hep-ph/0102122.

[57] J. L. Feng and K. T. Matchev, "Supersymmetry and the anomalous magnetic moment of the muon," *Phys. Rev. Lett.* **86** (2001) 3480–3483, arXiv:hep-ph/0102146.

[58] S. Coleman and J. Mandula, "All possible symmetries of the *s* matrix," *Phys. Rev.* **159** (Jul, 1967) 1251–1256. https://link.aps.org/doi/10.1103/PhysRev.159.1251.

[59] R. Haag, J. T. Lopuszanski, and M. Sohnius, "All Possible Generators of Supersymmetries of the s Matrix," *Nucl. Phys.* **B88** (1975) 257. [,257(1974)].

[60] J. Wess and B. Zumino, "Supergauge transformations in four dimensions," *Nucl. Phys. B* **70** (1974) 39.

[61] H. Georgi and S. L. Glashow, "Gauge theories without anomalies," *Phys. Rev. D* **6** (Jul, 1972) 429–431. https://link.aps.org/doi/10.1103/PhysRevD.6.429.

[62] S. Dimopoulos and D. W. Sutter, "The Supersymmetric flavor problem," *Nucl. Phys. B* **452** (1995) 496–512, arXiv:hep-ph/9504415.

[63] MEG Collaboration, T. Mori, "Final Results of the MEG Experiment," *Nuovo Cim. C* **39** no. 4, (2017) 325, arXiv:1606.08168 [hep-ex].

[64] H. P. Nilles, "Supersymmetry, Supergravity and Particle Physics," *Phys. Rept.* **110** (1984) 1–162.

[65] A. Lahanas and D. Nanopoulos, "The road to no-scale supergravity," *Physics Reports* **145** no. 1, (1987) 1 – 139. http://www.sciencedirect.com/science/article/pii/0370157387900342.

[66] J. L. Feng, A. Rajaraman, and F. Takayama, "Superweakly interacting massive particles," *Phys. Rev. Lett.* **91** (2003) 011302, arXiv:hep-ph/0302215.

[67] S. Y. Choi, J. Kalinowski, G. A. Moortgat-Pick, and P. M. Zerwas, "Analysis of the neutralino system in supersymmetric theories," *Eur. Phys. J. C* **22** (2001) 563–579, arXiv:hep-ph/0108117. [Addendum: Eur.Phys.J.C 23, 769–772 (2002)].

[68] Super-Kamiokande Collaboration, "Search for proton decay via $p \to e^+\pi^0$ and $p \to \mu^+\pi^0$ in 0.31 megaton-years exposure of the Super-Kamiokande water Cherenkov detector," *Phys. Rev.* **D95** no. 1, (2017) 012004, arXiv:1610.03597 [hep-ex].

[69] J. R. Ellis, "Beyond the standard model for hill walkers," in *1998 European School of High-Energy Physics*, pp. 133–196. 8, 1998. arXiv:hep-ph/9812235.

[70] J. R. Ellis, J. Hagelin, D. V. Nanopoulos, *et al.*, "Supersymmetric Relics from the Big Bang," *Nucl. Phys. B* **238** (1984) 453–476.

[71] D. O. Caldwell, R. M. Eisberg, D. M. Grumm, *et al.*, "Laboratory limits on galactic cold dark matter," *Phys. Rev. Lett.* **61** (Aug, 1988) 510–513. https://link.aps.org/doi/10.1103/PhysRevLett.61.510.

[72] M. Mori, M. M. Nojiri, K. S. Hirata, *et al.*, "Search for neutralino dark matter heavier than the *w* boson at kamiokande," *Phys. Rev. D* **48** (Dec, 1993) 5505–5518. https://link.aps.org/doi/10.1103/PhysRevD.48.5505.

[73] CDMS Collaboration, D. S. Akerib *et al.*, "Exclusion limits on the WIMP-nucleon cross section from the first run of the Cryogenic Dark Matter Search in the Soudan Underground Laboratory," *Phys. Rev. D* **72** (2005) 052009, arXiv:astro-ph/0507190.

[74] A. Djouadi, J.-L. Kneur, and G. Moultaka, "SuSpect: A Fortran code for the supersymmetric and Higgs particle spectrum in the MSSM," *Comput. Phys. Commun.* **176** (2007) 426–455, arXiv:hep-ph/0211331.

[75] C. F. Berger, J. S. Gainer, J. L. Hewett, and T. G. Rizzo, "Supersymmetry without prejudice," *Journal of High Energy Physics* **2009** no. 02, (Feb, 2009) 023–023. http://dx.doi.org/10.1088/1126-6708/2009/02/023.

[76] J. Alwall, P. Schuster, and N. Toro, "Simplified Models for a First Characterization of New Physics at the LHC," *Phys. Rev.* **D79** (2009) 075020, arXiv:0810.3921 [hep-ph].

[77] L. N. P. W. Group, "Simplified Models for LHC New Physics Searches," *J. Phys.* **G39** (2012) 105005, arXiv:1105.2838 [hep-ph].

[78] D. S. Alves, E. Izaguirre, and J. G. Wacker, "Where the Sidewalk Ends: Jets and Missing Energy Search Strategies for the 7 TeV LHC," *JHEP* **10** (2011) 012, arXiv:1102.5338 [hep-ph].

[79] F. Ambrogi, S. Kraml, S. Kulkarni, *et al.*, "On the coverage of the pMSSM by simplified model results," *Eur. Phys. J. C* **78** no. 3, (2018) 215, arXiv:1707.09036 [hep-ph].

[80] O. Buchmueller and J. Marrouche, "Universal mass limits on gluino and third-generation squarks in the context of Natural-like SUSY spectra," *Int. J. Mod. Phys. A* **29** no. 06, (2014) 1450032, arXiv:1304.2185 [hep-ph].

[81] W. Beenakker, C. Borschensky, M. Krämer, *et al.*, "NNLL-fast: predictions for coloured supersymmetric particle production at the LHC with threshold and Coulomb resummation," *JHEP* **12** (2016) 133, arXiv:1607.07741 [hep-ph].

[82] M. Beneke, M. Czakon, P. Falgari, *et al.*, "Threshold expansion of the $gg(q\bar{q}) \to Q\bar{Q} + X$ cross section at $\mathcal{O}(\alpha_s^4)$," *Phys. Lett. B* **690** (2010) 483, arXiv:0911.5166 [hep-ph].

[83] J. Fiaschi and M. Klasen, "Neutralino-chargino pair production at NLO+NLL with resummation-improved parton density functions for LHC Run II," *Phys. Rev. D* **98** no. 5, (2018) 055014, arXiv:1805.11322 [hep-ph].

[84] B. Fuks, M. Klasen, D. R. Lamprea, and M. Rothering, "Gaugino production in proton-proton collisions at a center-of-mass energy of 8 TeV," *JHEP* **10** (2012) 081, arXiv:1207.2159 [hep-ph].

[85] J. Fiaschi and M. Klasen, "Slepton pair production at the LHC in NLO+NLL with resummation-improved parton densities," *JHEP* **03** (2018) 094, arXiv:1801.10357 [hep-ph].

[86] ATLAS Collaboration, M. Aaboud *et al.*, "Dark matter interpretations of ATLAS searches for the electroweak production of supersymmetric particles in $\sqrt{s} = 8$ TeV proton-proton collisions," *JHEP* **09** (2016) 175, arXiv:1608.00872 [hep-ex].

[87] ATLAS Collaboration, "Summary of the ATLAS experiment's sensitivity to supersymmetry after LHC Run 1 — interpreted in the phenomenological MSSM," *JHEP* **10** (2015) 134, arXiv:1508.06608 [hep-ex].

[88] ATLAS Collaboration, "Mass reach of the atlas searches for supersymmetry." https://atlas.web.cern.ch/Atlas/GROUPS/PHYSICS/PUBNOTES/ATL-PHYS-PUB-2020-020/fig_23.png, 2020.

[89] CMS Collaboration, "Summary plot moriond 2017." https://twiki.cern.ch/twiki/pub/CMSPublic/SUSYSummary2017/Moriond2017_BarPlot.pdf, 2017.

[90] L. S. W. Group, "Notes lepsusywg/02-04.1 and lepsusywg/01-03.1." http://lepsusy.web.cern.ch/lepsusy/, 2004. Accessed: 2021-02-11.

[91] ATLAS Collaboration, "Searches for electroweak production of supersymmetric particles with compressed mass spectra in $\sqrt{s} = 13$ TeV pp collisions with the ATLAS detector," *Phys. Rev. D* **101** (2020) 052005, arXiv:1911.12606 [hep-ex].

[92] ATLAS Collaboration, "Observation of a new particle in the search for the Standard Model Higgs boson with the ATLAS detector at the LHC," *Phys. Lett. B* **716** (2012) 1–29, arXiv:1207.7214 [hep-ex].

[93] CMS Collaboration, "Observation of a New Boson at a Mass of 125 GeV with the CMS Experiment at the LHC," *Phys. Lett. B* **716** (2012) 30–61, arXiv:1207.7235 [hep-ex].

[94] A. Buckley, "PySLHA: a Pythonic interface to SUSY Les Houches Accord data," *Eur. Phys. J. C* **75** no. 10, (2015) 467, arXiv:1305.4194 [hep-ph].

[95] CERN, "About cern." https://home.cern/about. Accessed: 2021-01-21.

[96] CERN, "CERN Annual report 2019," tech. rep., CERN, Geneva, 2020. https://cds.cern.ch/record/2723123.

[97] O. S. Bruning, P. Collier, P. Lebrun, *et al.*, *LHC Design Report*. CERN Yellow Reports: Monographs. CERN, Geneva, 2004. https://cds.cern.ch/record/782076.

[98] M. Blewett and N. Vogt-Nilsen, "Proceedings of the 8th international conference on high-energy accelerators, cern 1971. conference held at geneva, 20–24 september 1971.," tech. rep., 1971, 1971.

[99] L. R. Evans and P. Bryant, "LHC Machine," *JINST* **3** (2008) S08001. 164 p. http://cds.cern.ch/record/1129806. This report is an abridged version of the LHC Design Report (CERN-2004-003).

[100] R. Scrivens, M. Kronberger, D. Küchler, *et al.*, "Overview of the status and developments on primary ion sources at CERN*,". https://cds.cern.ch/record/1382102.

[101] M. Vretenar, J. Vollaire, R. Scrivens, *et al.*, *Linac4 design report*, vol. 6 of *CERN Yellow Reports: Monographs*. CERN, Geneva, 2020. https://cds.cern.ch/record/2736208.

[102] E. Mobs, "The CERN accelerator complex - 2019. Complexe des accélérateurs du CERN - 2019,". https://cds.cern.ch/record/2684277. General Photo.

[103] ATLAS Collaboration, "The ATLAS Experiment at the CERN Large Hadron Collider," *JINST* **3** (2008) S08003.

[104] CMS Collaboration, "The CMS Experiment at the CERN LHC," *JINST* **3** (2008) S08004.

[105] ALICE Collaboration, "The ALICE experiment at the CERN LHC," *JINST* **3** (2008) S08002.

[106] LHCb Collaboration, "The LHCb Detector at the LHC," *JINST* **3** (2008) S08005.

[107] TOTEM Collaboration, "The TOTEM experiment at the CERN Large Hadron Collider," *JINST* **3** (2008) S08007.

[108] LHCf Collaboration, "Technical design report of the LHCf experiment: Measurement of photons and neutral pions in the very forward region of LHC,".

[109] MoEDAL Collaboration, "Technical Design Report of the MoEDAL Experiment,".

[110] ATLAS Collaboration, "ATLAS Public Results - Luminosity Public Results Run 2,". https://twiki.cern.ch/twiki/bin/view/AtlasPublic/LuminosityPublicResultsRun2. Accessed: 2021-01-17.

[111] ATLAS Collaboration, Z. Marshall, "Simulation of Pile-up in the ATLAS Experiment," *J. Phys. Conf. Ser.* **513** (2014) 022024.

[112] "First beam in the LHC - accelerating science,". https://home.cern/news/news/accelerators/record-luminosity-well-done-lhc. Accessed: 2021-01-10.

[113] ATLAS Collaboration, "Luminosity determination in pp collisions at $\sqrt{s}$ = 13 TeV using the ATLAS detector at the LHC," Tech. Rep. ATLAS-CONF-2019-021, CERN, Geneva, Jun, 2019. https://cds.cern.ch/record/2677054.

[114] ATLAS Collaboration, "Luminosity determination in pp collisions at $\sqrt{s}$ = 8 TeV using the ATLAS detector at the LHC," *Eur. Phys. J. C* **76** no. 12, (2016) 653, arXiv:1608.03953 [hep-ex].

[115] G. Avoni, M. Bruschi, G. Cabras, *et al.*, "The new LUCID-2 detector for luminosity measurement and monitoring in ATLAS," *Journal of Instrumentation* **13** no. 07, (Jul, 2018) P07017–P07017. https://doi.org/10.1088/1748-0221/13/07/p07017.

[116] S. van der Meer, "Calibration of the effective beam height in the ISR," Tech. Rep. CERN-ISR-PO-68-31. ISR-PO-68-31, CERN, Geneva, 1968. https://cds.cern.ch/record/296752.

[117] P. Grafström and W. Kozanecki, "Luminosity determination at proton colliders," *Progress in Particle and Nuclear Physics* **81** (2015) 97 – 148. http://www.sciencedirect.com/science/article/pii/S0146641014000878.

[118] M. Bajko *et al.*, "Report of the Task Force on the Incident of 19th September 2008 at the LHC," Tech. Rep. LHC-PROJECT-Report-1168. CERN-LHC-PROJECT-Report-1168, CERN, Geneva, Mar, 2009. https://cds.cern.ch/record/1168025.

[119] "New schedule for CERN's accelerators and experiments,". https://home.cern/news/press-release/cern/first-beam-lhc-accelerating-science. Accessed: 2021-01-10.

[120] ATLAS Collaboration, "Luminosity Determination in pp Collisions at $\sqrt{s}$ = 7 TeV Using the ATLAS Detector at the LHC," *Eur. Phys. J. C* **71** (2011) 1630, arXiv:1101.2185 [hep-ex].

[121] ATLAS Collaboration, "Improved luminosity determination in pp collisions at $\sqrt{s}$ = 7 TeV using the ATLAS detector at the LHC.," *Eur. Phys. J. C* **73** no. CERN-PH-EP-2013-026, (Feb, 2013) 2518. 27 p. https://cds.cern.ch/record/1517411.

[122] "Record luminosity: well done LHC,". https://home.cern/news/news/accelerators/new-schedule-cerns-accelerators-and-experiments. Accessed: 2021-01-10.

[123] CERN, "New schedule for CERN's accelerators and experiments," November, 2020. https://home.cern/news/news/accelerators/new-schedule-cerns-accelerators-and-experiments. Accessed: 2021-03-12.

[124] A. G., B. A. I., B. O., *et al.*, *High-Luminosity Large Hadron Collider (HL-LHC): Technical Design Report V. 0.1*. CERN Yellow Reports: Monographs. CERN, Geneva, 2017. https://cds.cern.ch/record/2284929.

[125] J. Pequenao, "Computer generated image of the whole ATLAS detector." Mar, 2008.

[126] ATLAS Collaboration, "ATLAS: Detector and physics performance technical design report. Volume 1,".

[127] J. Pequenao, "Computer generated image of the ATLAS inner detector." Mar, 2008.

[128] ATLAS Collaboration, K. Potamianos, "The upgraded Pixel detector and the commissioning of the Inner Detector tracking of the ATLAS experiment for Run-2 at the Large Hadron Collider," Tech. Rep. ATL-PHYS-PROC-2016-104, CERN, Geneva, Aug, 2016. https://cds.cern.ch/record/2209070. 15 pages, EPS-HEP 2015 Proceedings.

[129] ATLAS IBL Collaboration, "Production and Integration of the ATLAS Insertable B-Layer," *JINST* **13** no. 05, (2018) T05008, arXiv:1803.00844 [physics.ins-det].

[130] ATLAS Collaboration, "ATLAS Insertable B-Layer Technical Design Report," Tech. Rep. CERN-LHCC-2010-013. ATLAS-TDR-19, Sep, 2010. http://cds.cern.ch/record/1291633.

[131] ATLAS Collaboration, "ATLAS b-jet identification performance and efficiency measurement with $t\bar{t}$ events in pp collisions at $\sqrt{s}$ = 13 TeV," *Eur. Phys. J. C* **79** no. 11, (2019) 970, arXiv:1907.05120 [hep-ex].

[132] ATLAS Collaboration, "Particle Identification Performance of the ATLAS Transition Radiation Tracker." ATLAS-CONF-2011-128, 2011. https://cds.cern.ch/record/1383793.

[133] J. Pequenao, "Computer Generated image of the ATLAS calorimeter." Mar, 2008.

[134] J. Pequenao, "Computer generated image of the ATLAS Muons subsystem." Mar, 2008.

[135] S. Lee, M. Livan, and R. Wigmans, "Dual-Readout Calorimetry," *Rev. Mod. Phys.* **90** no. arXiv:1712.05494. 2, (Dec, 2017) 025002. 40 p. https://cds.cern.ch/record/2637852. 44 pages, 53 figures, accepted for publication in Review of Modern Physics.

[136] M. Leite, "Performance of the ATLAS Zero Degree Calorimeter," Tech. Rep. ATL-FWD-PROC-2013-001, CERN, Geneva, Nov, 2013. https://cds.cern.ch/record/1628749.

[137] S. Abdel Khalek *et al.*, "The ALFA Roman Pot Detectors of ATLAS," *JINST* **11** no. 11, (2016) P11013, arXiv:1609.00249 [physics.ins-det].

[138] U. Amaldi, G. Cocconi, A. Diddens, *et al.*, "The real part of the forward proton proton scattering amplitude measured at the cern intersecting storage rings," *Physics Letters B* **66** no. 4, (1977) 390 – 394. http://www.sciencedirect.com/science/article/pii/0370269377900223.

[139] L. Adamczyk, E. Banaś, A. Brandt, *et al.*, "Technical Design Report for the ATLAS Forward Proton Detector," Tech. Rep. CERN-LHCC-2015-009. ATLAS-TDR-024, May, 2015. https://cds.cern.ch/record/2017378.

[140] ATLAS Collaboration, A. R. Martínez, "The Run-2 ATLAS Trigger System," *J. Phys. Conf. Ser.* **762** no. 1, (2016) 012003.

[141] ATLAS Collaboration, *ATLAS level-1 trigger: Technical Design Report.* Technical Design Report ATLAS. CERN, Geneva, 1998. https://cds.cern.ch/record/381429.

[142] ATLAS Collaboration, "Operation of the ATLAS trigger system in Run 2," *JINST* **15** no. 10, (2020) P10004, arXiv:2007.12539 [physics.ins-det].

[143] ATLAS Collaboration, P. Jenni, M. Nessi, M. Nordberg, and K. Smith, *ATLAS high-level trigger, data-acquisition and controls: Technical Design Report.* Technical Design Report ATLAS. CERN, Geneva, 2003. https://cds.cern.ch/record/616089.

[144] ATLAS Collaboration, "The ATLAS Simulation Infrastructure," *Eur. Phys. J. C* **70** (2010) 823–874, arXiv:1005.4568 [physics.ins-det].

[145] T. Gleisberg, S. Hoeche, F. Krauss, *et al.*, "Event generation with SHERPA 1.1," *JHEP* **02** (2009) 007, arXiv:0811.4622 [hep-ph].

[146] A. Buckley *et al.*, "General-purpose event generators for LHC physics," *Phys. Rept.* **504** (2011) 145–233, arXiv:1101.2599 [hep-ph].

[147] V. N. Gribov and L. N. Lipatov, "Deep inelastic e p scattering in perturbation theory," *Sov. J. Nucl. Phys.* **15** (1972) 438–450.

[148] J. Blumlein, T. Doyle, F. Hautmann, *et al.*, "Structure functions in deep inelastic scattering at HERA," in *Workshop on Future Physics at HERA (To be followed by meetings 7-9 Feb and 30-31 May 1996 at DESY)*. 9, 1996. arXiv:hep-ph/9609425.

[149] A. Buckley, J. Ferrando, S. Lloyd, *et al.*, "LHAPDF6: parton density access in the LHC precision era," *Eur. Phys. J. C* **75** (2015) 132, arXiv:1412.7420 [hep-ph].

[150] M. Bengtsson and T. Sjostrand, "Coherent Parton Showers Versus Matrix Elements: Implications of PETRA - PEP Data," *Phys. Lett. B* **185** (1987) 435.

[151] S. Catani, F. Krauss, R. Kuhn, and B. R. Webber, "QCD matrix elements + parton showers," *JHEP* **11** (2001) 063, arXiv:hep-ph/0109231.

[152] L. Lonnblad, "Correcting the color dipole cascade model with fixed order matrix elements," *JHEP* **05** (2002) 046, arXiv:hep-ph/0112284.

[153] B. Andersson, G. Gustafson, G. Ingelman, and T. Sjostrand, "Parton Fragmentation and String Dynamics," *Phys. Rept.* **97** (1983) 31–145.

[154] B. Andersson, *The Lund Model*. Cambridge Monographs on Particle Physics, Nuclear Physics and Cosmology. Cambridge University Press, 1998.

[155] D. Amati and G. Veneziano, "Preconfinement as a Property of Perturbative QCD," *Phys. Lett. B* **83** (1979) 87–92.

[156] D. Yennie, S. Frautschi, and H. Suura, "The infrared divergence phenomena and high-energy processes," *Annals of Physics* **13** no. 3, (1961) 379–452. https://www.sciencedirect.com/science/article/pii/0003491661901518.

[157] M. Dobbs and J. B. Hansen, "The HepMC C++ Monte Carlo event record for High Energy Physics," *Comput. Phys. Commun.* **134** (2001) 41–46.

[158] GEANT4 Collaboration, "GEANT4: A Simulation toolkit," *Nucl. Instrum. Meth.* **A506** (2003) 250–303.

[159] ATLAS Collaboration, "The new Fast Calorimeter Simulation in ATLAS," Tech. Rep. ATL-SOFT-PUB-2018-002, CERN, Geneva, Jul, 2018. https://cds.cern.ch/record/2630434.

[160] K. Cranmer, "Practical Statistics for the LHC," in *2011 European School of High-Energy Physics*, pp. 267–308. 2014. arXiv:1503.07622 [physics.data-an].

[161] G. Cowan, K. Cranmer, E. Gross, and O. Vitells, "Asymptotic formulae for likelihood-based tests of new physics," *Eur. Phys. J.* **C71** (2011) 1554, arXiv:1007.1727 [physics.data-an]. [Erratum: Eur. Phys. J.C73,2501(2013)].

[162] ATLAS Collaboration, "Reproduction searches for new physics with the ATLAS experiment through publication of full statistical likelihoods." ATL-PHYS-PUB-2019-029, 2019. https://cds.cern.ch/record/2684863.

[163] ROOT Collaboration, K. Cranmer, G. Lewis, L. Moneta, *et al.*, "HistFactory: A tool for creating statistical models for use with RooFit and RooStats," Tech. Rep. CERN-OPEN-2012-016, New York U., New York, Jan, 2012. https://cds.cern.ch/record/1456844.

[164] W. Verkerke and D. P. Kirkby, "The RooFit toolkit for data modeling," *eConf* **C0303241** (2003) MOLT007, arXiv:physics/0306116 [physics]. [,186(2003)].

[165] F. James and M. Roos, "MINUIT: a system for function minimization and analysis of the parameter errors and corrections," *Comput. Phys. Commun.* **10** no. CERN-DD-75-20, (Jul, 1975) 343–367. 38 p. https://cds.cern.ch/record/310399.

[166] L. Moneta, K. Belasco, K. S. Cranmer, *et al.*, "The RooStats Project," *PoS* **ACAT2010** (2010) 057, arXiv:1009.1003 [physics.data-an].

[167] R. Brun and F. Rademakers, "ROOT: An object oriented data analysis framework," *Nucl. Instrum. Meth.* **A389** (1997) 81–86.

[168] I. Antcheva *et al.*, "ROOT — A C++ framework for petabyte data storage, statistical analysis and visualization," *Computer Physics Communications* **182** no. 6, (2011) 1384 – 1385. http://www.sciencedirect.com/science/article/pii/S0010465511000701.

[169] M. Baak, G. J. Besjes, D. Côte, A. Koutsman, J. Lorenz, D. Short, "HistFitter software framework for statistical data analysis," *Eur. Phys. J.* **C75** (2015) 153, arXiv:1410.1280 [hep-ex].

[170] L. Heinrich, M. Feickert, G. Stark, and K. Cranmer, "pyhf: pure-python implementation of histfactory statistical models," *Journal of Open Source Software* **6** no. 58, (2021) 2823. https://doi.org/10.21105/joss.02823.

[171] L. Heinrich, M. Feickert, and G. Stark, "pyhf: v0.6.0," Version 0.6.0. https://github.com/scikit-hep/pyhf.

[172] C. R. Harris, K. J. Millman, S. J. van der Walt, *et al.*, "Array programming with NumPy," *Nature* **585** no. 7825, (Sept., 2020) 357–362. https://doi.org/10.1038/s41586-020-2649-2.

[173] A. Paszke, S. Gross, F. Massa, *et al.*, "Pytorch: An imperative style, high-performance deep learning library," in *Advances in Neural Information Processing Systems 32*, H. Wallach, H. Larochelle, A. Beygelzimer, *et al.*, eds., pp. 8024–8035. Curran Associates, Inc., 2019. http://papers.neurips.cc/paper/9015-pytorch-an-imperative-style-high-performance-deep-learning-library.pdf.

[174] M. Abadi, A. Agarwal, P. Barham, *et al.*, "TensorFlow: Large-scale machine learning on heterogeneous systems," 2015. https://www.tensorflow.org/. Software available from tensorflow.org.

[175] J. Bradbury, R. Frostig, P. Hawkins, *et al.*, "JAX: composable transformations of Python+NumPy programs," Version 0.1.46, 2018. http://github.com/google/jax.

[176] S. S. Wilks, "The large-sample distribution of the likelihood ratio for testing composite hypotheses," *Ann. Math. Statist.* **9** no. 1, (03, 1938) 60–62. https://doi.org/10.1214/aoms/1177732360.

[177] A. Wald, "Tests of statistical hypotheses concerning several parameters when the number of observations is large," *Transactions of the American Mathematical Society* **54** no. 3, (1943) 426–482. https://doi.org/10.1090/S0002-9947-1943-0012401-3.

[178] G. Cowan, "Statistics for Searches at the LHC," in *69th Scottish Universities Summer School in Physics: LHC Physics*, pp. 321–355. 7, 2013. arXiv:1307.2487 [hep-ex].

[179] A. L. Read, "Presentation of search results: the CL_S technique," *J. Phys. G* **28** (2002) 2693.

[180] R. D. Cousins, J. T. Linnemann, and J. Tucker, "Evaluation of three methods for calculating statistical significance when incorporating a systematic uncertainty into a test of the background-only hypothesis for a Poisson process," *Nucl. Instrum. Meth. A* **595** no. 2, (2008) 480, arXiv:physics/0702156 [physics.data-an].

[181] K. Cranmer, "Statistical challenges for searches for new physics at the LHC," in *Statistical Problems in Particle Physics, Astrophysics and Cosmology (PHYSTAT 05): Proceedings, Oxford, UK, September 12-15, 2005*, pp. 112–123. 2005. arXiv:physics/0511028 [physics.data-an]. http://www.physics.ox.ac.uk/phystat05/proceedings/files//Cranmer_LHCStatisticalChallenges.ps.

[182] ATLAS Collaboration, "Search for direct pair production of a chargino and a neutralino decaying to the 125 GeV Higgs boson in $\sqrt{s} = 8$ TeV pp collisions with the ATLAS detector," *Eur. Phys. J. C* **75** (2015) 208, arXiv:1501.07110 [hep-ex].

[183] ATLAS Collaboration, "Search for chargino and neutralino production in final states with a Higgs boson and missing transverse momentum at $\sqrt{s} = 13$ TeV with the ATLAS detector," *Phys. Rev. D* **100** (2019) 012006, arXiv:1812.09432 [hep-ex].

[184] CMS Collaboration, "Search for electroweak production of charginos and neutralinos in WH events in proton–proton collisions at $\sqrt{s} = 13$ TeV," *JHEP* **11** (2017) 029, arXiv:1706.09933 [hep-ex].

[185] ATLAS Collaboration, "Search for direct production of electroweakinos in final states with one lepton, missing transverse momentum and a Higgs boson decaying into two b-jets in pp collisions at $\sqrt{s} = 13$ TeV with the ATLAS detector," *Eur. Phys. J. C* **80** (2020) 691, arXiv:1909.09226 [hep-ex].

[186] ATLAS Collaboration, "Improvements in $t\bar{t}$ modelling using NLO+PS Monte Carlo generators for Run 2." ATL-PHYS-PUB-2018-009, 2018. https://cds.cern.ch/record/2630327.

[187] ATLAS Collaboration, "Modelling of the $t\bar{t}H$ and $t\bar{t}V(V = W, Z)$ processes for $\sqrt{s} = 13$ TeV ATLAS analyses." ATL-PHYS-PUB-2016-005, 2016. https://cds.cern.ch/record/2120826.

[188] ATLAS Collaboration, "ATLAS simulation of boson plus jets processes in Run 2." ATL-PHYS-PUB-2017-006, 2017. https://cds.cern.ch/record/2261937.

[189] ATLAS Collaboration, "Multi-Boson Simulation for 13 TeV ATLAS Analyses." ATL-PHYS-PUB-2017-005, 2017. https://cds.cern.ch/record/2261933.

[190] J. Alwall, R. Frederix, S. Frixione, *et al.*, "The automated computation of tree-level and next-to-leading order differential cross sections, and their matching to parton shower simulations," *JHEP* **07** (2014) 079, arXiv:1405.0301 [hep-ph].

[191] R. Frederix and S. Frixione, "Merging meets matching in MC@NLO," *JHEP* **12** (2012) 061, arXiv:1209.6215 [hep-ph].

[192] "Parton distributions with LHC data," *Nucl. Phys. B* **867** (2013) 244, arXiv:1207.1303 [hep-ph].

[193] T. Sjöstrand, S. Ask, J. R. Christiansen, *et al.*, "An Introduction to PYTHIA 8.2," *Comput. Phys. Commun.* **191** (2015) 159–177, arXiv:1410.3012 [hep-ph].

[194] ATLAS Collaboration, "ATLAS Pythia 8 tunes to 7 TeV data." ATL-PHYS-PUB-2014-021, 2014. https://cds.cern.ch/record/1966419.

[195] L. Lönnblad and S. Prestel, "Matching tree-level matrix elements with interleaved showers," *JHEP* **03** (2012) 019, arXiv:1109.4829 [hep-ph].

[196] D. J. Lange, "The EvtGen particle decay simulation package," *Nucl. Instrum. Meth. A* **462** (2001) 152.

[197] ATLAS Collaboration, "The Pythia 8 A3 tune description of ATLAS minimum bias and inelastic measurements incorporating the Donnachie–Landshoff diffractive model." ATL-PHYS-PUB-2016-017, 2016. https://cds.cern.ch/record/2206965.

[198] B. Fuks, M. Klasen, D. R. Lamprea, and M. Rothering, "Precision predictions for electroweak superpartner production at hadron colliders with RESUMMINO," *Eur. Phys. J. C* **73** (2013) 2480, arXiv:1304.0790 [hep-ph].

[199] S. Alioli, P. Nason, C. Oleari, and E. Re, "A general framework for implementing NLO calculations in shower Monte Carlo programs: the POWHEG BOX," *JHEP* **06** (2010) 043, arXiv:1002.2581 [hep-ph].

[200] S. Frixione, P. Nason, and G. Ridolfi, "A Positive-weight next-to-leading-order Monte Carlo for heavy flavour hadroproduction," *JHEP* **09** (2007) 126, arXiv:0707.3088 [hep-ph].

[201] P. Nason, "A New method for combining NLO QCD with shower Monte Carlo algorithms," *JHEP* **11** (2004) 040, arXiv:hep-ph/0409146.

[202] E. Bothmann *et al.*, "Event generation with Sherpa 2.2," *SciPost Phys.* **7** no. 3, (2019) 034, arXiv:1905.09127 [hep-ph].

[203] NNPDF Collaboration, "Parton distributions for the LHC run II," *JHEP* **04** (2015) 040, arXiv:1410.8849 [hep-ph].

[204] M. Czakon and A. Mitov, "Top++: A program for the calculation of the top-pair cross-section at hadron colliders," *Comput. Phys. Commun.* **185** (2014) 2930, arXiv:1112.5675 [hep-ph].

[205] M. Cacciari, M. Czakon, M. Mangano, *et al.*, "Top-pair production at hadron colliders with next-to-next-to-leading logarithmic soft-gluon resummation," *Phys. Lett. B* **710** (2012) 612–622, arXiv:1111.5869 [hep-ph].

[206] P. Kant, O. M. Kind, T. Kintscher, *et al.*, "HatHor for single top-quark production: Updated predictions and uncertainty estimates for single top-quark production in hadronic collisions," *Comput. Phys. Commun.* **191** (2015) 74–89, arXiv:1406.4403 [hep-ph].

[207] N. Kidonakis, "Two-loop soft anomalous dimensions for single top quark associated production with a W^- or H^-," *Phys. Rev. D* **82** (2010) 054018, arXiv:1005.4451 [hep-ph].

[208] J. M. Campbell and R. K. Ellis, "$t\bar{t}W^{+-}$ production and decay at NLO," *JHEP* **07** (2012) 052, arXiv:1204.5678 [hep-ph].

[209] A. Lazopoulos, T. McElmurry, K. Melnikov, and F. Petriello, "Next-to-leading order QCD corrections to $t\bar{t}Z$ production at the LHC," *Phys. Lett. B* **666** (2008) 62–65, arXiv:0804.2220 [hep-ph].

[210] R. Gavin, Y. Li, F. Petriello, and S. Quackenbush, "FEWZ 2.0: A code for hadronic Z production at next-to-next-to-leading order," arXiv:1011.3540 [hep-ph].

[211] LHC Higgs Cross Section Working Group Collaboration, "Handbook of LHC Higgs Cross Sections: 4. Deciphering the Nature of the Higgs Sector," arXiv:1610.07922 [hep-ph].

[212] ATLAS Collaboration, "Example ATLAS tunes of PYTHIA8, PYTHIA6 and POWHEG to an observable sensitive to Z boson transverse momentum." ATL-PHYS-PUB-2013-017, 2013. https://cds.cern.ch/record/1629317.

[213] ATLAS Collaboration, "Performance of the ATLAS track reconstruction algorithms in dense environments in LHC Run 2," *Eur. Phys. J. C* **77** (2017) 673, arXiv:1704.07983 [hep-ex].

[214] R. Frühwirth, "Application of Kalman filtering to track and vertex fitting," *Nucl. Instrum. Methods Phys. Res., A* **262** no. HEPHY-PUB-503, (Jun, 1987) 444. 19 p. https://cds.cern.ch/record/178627.

[215] T. Cornelissen, M. Elsing, I. Gavrilenko, *et al.*, "The new ATLAS track reconstruction (NEWT)," *J. Phys.: Conf. Ser.* **119** (2008) 032014. https://cds.cern.ch/record/1176900.

[216] ATLAS Collaboration, "Vertex Reconstruction Performance of the ATLAS Detector at $\sqrt{s}$ = 13 TeV." ATL-PHYS-PUB-2015-026, 2015. https://cds.cern.ch/record/2037717.

[217] ATLAS Collaboration, "Reconstruction of primary vertices at the ATLAS experiment in Run 1 proton–proton collisions at the LHC," *Eur. Phys. J. C* **77** (2017) 332, arXiv:1611.10235 [hep-ex].

[218] ATLAS Collaboration, "Topological cell clustering in the ATLAS calorimeters and its performance in LHC Run 1," *Eur. Phys. J. C* **77** (2017) 490, arXiv:1603.02934 [hep-ex].

[219] ATLAS Collaboration, "Electron and photon performance measurements with the ATLAS detector using the 2015–2017 LHC proton–proton collision data," *JINST* **14** (2019) P12006, arXiv:1908.00005 [hep-ex].

[220] ATLAS Collaboration, "Measurement of the photon identification efficiencies with the ATLAS detector using LHC Run 2 data collected in 2015 and 2016," *Eur. Phys. J. C* **79** (2019) 205, arXiv:1810.05087 [hep-ex].

[221] ATLAS Collaboration, "Electron reconstruction and identification in the ATLAS experiment using the 2015 and 2016 LHC proton–proton collision data at $\sqrt{s}$ = 13 TeV," *Eur. Phys. J. C* **79** (2019) 639, arXiv:1902.04655 [hep-ex].

[222] ATLAS Collaboration, "Muon reconstruction performance of the ATLAS detector in proton–proton collision data at $\sqrt{s}$ = 13 TeV," *Eur. Phys. J. C* **76** (2016) 292, arXiv:1603.05598 [hep-ex].

[223] ATLAS Collaboration, "Muon reconstruction and identification efficiency in ATLAS using the full Run 2 *pp* collision data set at $\sqrt{s}$ = 13 TeV," arXiv:2012.00578 [hep-ex].

[224] M. Cacciari, G. P. Salam, and G. Soyez, "The anti-k_t jet clustering algorithm," *JHEP* **04** (2008) 063, arXiv:0802.1189 [hep-ph].

[225] M. Cacciari, G. P. Salam, and G. Soyez, "FastJet user manual," *Eur. Phys. J. C* **72** (2012) 1896, arXiv:1111.6097 [hep-ph].

[226] M. Cacciari, "FastJet: A Code for fast k_t clustering, and more," in *Deep inelastic scattering. Proceedings, 14th International Workshop, DIS 2006, Tsukuba, Japan, April 20-24, 2006*, pp. 487–490. 2006. arXiv:hep-ph/0607071 [hep-ph]. [,125(2006)].

[227] ATLAS Collaboration, "Jet energy scale and resolution measured in proton-proton collisions at $\sqrt{s}$ = 13 TeV with the ATLAS detector," arXiv:2007.02645 [hep-ex].

[228] M. Cacciari and G. P. Salam, "Pileup subtraction using jet areas," *Phys. Lett. B* **659** (2008) 119–126, arXiv:0707.1378 [hep-ph].

[229] ATLAS Collaboration, "Jet energy measurement with the ATLAS detector in proton–proton collisions at $\sqrt{s}$ = 7 TeV," *Eur. Phys. J. C* **73** (2013) 2304, arXiv:1112.6426 [hep-ex].

[230] ATLAS Collaboration, "Determination of jet calibration and energy resolution in proton–proton collisions at $\sqrt{s}$ = 8 TeV using the ATLAS detector," arXiv:1910.04482 [hep-ex].

[231] ATLAS Collaboration, "Performance of pile-up mitigation techniques for jets in *pp* collisions at $\sqrt{s}$ = 8 TeV using the ATLAS detector," *Eur. Phys. J. C* **76** (2016) 581, arXiv:1510.03823 [hep-ex].

[232] ATLAS Collaboration, "Optimisation and performance studies of the ATLAS *b*-tagging algorithms for the 2017-18 LHC run." ATL-PHYS-PUB-2017-013, 2017. https://cds.cern.ch/record/2273281.

[233] ATLAS Collaboration, "ATLAS b-jet identification performance and efficiency measurement with $t\bar{t}$ events in pp collisions at $\sqrt{s} = 13$ TeV," *Eur. Phys. J. C* **79** (2019) 970, arXiv:1907.05120 [hep-ex].

[234] ATLAS Collaboration, "Measurements of b-jet tagging efficiency with the ATLAS detector using $t\bar{t}$ events at $\sqrt{s} = 13$ TeV," *JHEP* **08** (2018) 089, arXiv:1805.01845 [hep-ex].

[235] ATLAS Collaboration, "Performance of missing transverse momentum reconstruction with the ATLAS detector using proton–proton collisions at $\sqrt{s} = 13$ TeV," *Eur. Phys. J. C* **78** (2018) 903, arXiv:1802.08168 [hep-ex].

[236] ATLAS Collaboration, "$E_{\mathrm{T}}^{\mathrm{miss}}$ performance in the ATLAS detector using 2015-2016 LHC p-p collisions," Tech. Rep. ATLAS-CONF-2018-023, CERN, Geneva, Jun, 2018. http://cds.cern.ch/record/2625233.

[237] D. Adams *et al.*, "Recommendations of the Physics Objects and Analysis Harmonisation Study Groups 2014," Tech. Rep. ATL-PHYS-INT-2014-018, CERN, Geneva, Jul, 2014. https://cds.cern.ch/record/1743654.

[238] M. Cacciari, G. P. Salam, and G. Soyez, "The Catchment Area of Jets," *JHEP* **04** (2008) 005, arXiv:0802.1188 [hep-ph].

[239] UA1 Collaboration, "Experimental Observation of Isolated Large Transverse Energy Electrons with Associated Missing Energy at $\sqrt{s} = 540$ GeV," *Phys. Lett. B* **122** (1983) 103–116.

[240] Aachen-Annecy-Birmingham-CERN-Helsinki-London(QMC)-Paris(CdF)-Riverside-Rome-Rutherford-Saclay(CEN)-Vienna Collaboration, G. Arnison *et al.*, "Further evidence for charged intermediate vector bosons at the SPS collider," *Phys. Lett. B* **129** no. CERN-EP-83-111, (Jun, 1985) 273–282. 17 p. https://cds.cern.ch/record/163856.

[241] U. Baur, "Measuring the W boson mass at hadron colliders," in *Mini-Workshop on Electroweak Precision Data and the Higgs Mass*. 4, 2003. arXiv:hep-ph/0304266.

[242] J. Smith, W. L. van Neerven, and J. A. M. Vermaseren, "The Transverse Mass and Width of the W Boson," *Phys. Rev. Lett.* **50** (1983) 1738.

[243] D. R. Tovey, "On measuring the masses of pair-produced semi-invisibly decaying particles at hadron colliders," *JHEP* **04** (2008) 034, arXiv:0802.2879 [hep-ph].

[244] G. Polesello and D. R. Tovey, "Supersymmetric particle mass measurement with the boost-corrected contransverse mass," *JHEP* **03** (2010) 030, arXiv:0910.0174 [hep-ph].

[245] ATLAS Collaboration, "Performance of the missing transverse momentum triggers for the ATLAS detector during Run-2 data taking," *JHEP* **08** (2020) 080, arXiv:2005.09554 [hep-ex].

[246] ATLAS Collaboration, "Performance of algorithms that reconstruct missing transverse momentum in $\sqrt{s} = 8$ TeV proton-proton collisions in the ATLAS detector," *Eur. Phys. J. C* **77** no. 4, (2017) 241, arXiv:1609.09324 [hep-ex].

[247] ATLAS Collaboration, "ATLAS data quality operations and performance for 2015–2018 data-taking," *JINST* **15** (2020) P04003, arXiv:1911.04632 [physics.ins-det].

[248] ATLAS Collaboration, "Selection of jets produced in 13 TeV proton–proton collisions with the ATLAS detector." ATLAS-CONF-2015-029, 2015. https://cds.cern.ch/record/2037702.

[249] N. Hartmann, "ahoi." https://gitlab.com/nikoladze/ahoi, 2018.

[250] ATLAS Collaboration, "Object-based missing transverse momentum significance in the ATLAS detector," Tech. Rep. ATLAS-CONF-2018-038, CERN, Geneva, Jul, 2018. https://cds.cern.ch/record/2630948.

[251] A. Roodman, "Blind analysis in particle physics," *eConf* **C030908** (2003) TUIT001, arXiv:physics/0312102.

[252] W. Buttinger, "Using Event Weights to account for differences in Instantaneous Luminosity and Trigger Prescale in Monte Carlo and Data," tech. rep., CERN, Geneva, May, 2015. https://cds.cern.ch/record/2014726.

[253] ATLAS Collaboration, "Measurement of the Inelastic Proton–Proton Cross Section at $\sqrt{s}$ = 13 TeV with the ATLAS Detector at the LHC," *Phys. Rev. Lett.* **117** (2016) 182002, arXiv:1606.02625 [hep-ex].

[254] ATLAS Collaboration, "A method for the construction of strongly reduced representations of ATLAS experimental uncertainties and the application thereof to the jet energy scale." ATL-PHYS-PUB-2015-014, 2015. https://cds.cern.ch/record/2037436.

[255] J. Bellm *et al.*, "Herwig 7.0/Herwig++ 3.0 release note," *Eur. Phys. J.* **C76** no. 4, (2016) 196, arXiv:1512.01178 [hep-ph].

[256] ATLAS Collaboration, "Simulation of top-quark production for the ATLAS experiment at $\sqrt{s}$ = 13 TeV." ATL-PHYS-PUB-2016-004, 2016. https://cds.cern.ch/record/2120417.

[257] S. Frixione, E. Laenen, P. Motylinski, *et al.*, "Single-top hadroproduction in association with a W boson," *JHEP* **07** (2008) 029, arXiv:0805.3067 [hep-ph].

[258] ATLAS Collaboration, "SUSY July 2020 Summary Plot Update," Tech. Rep. ATL-PHYS-PUB-2020-020, CERN, Geneva, Jul, 2020. http://cds.cern.ch/record/2725258.

[259] CMS Collaboration, "Search for chargino-neutralino production in final states with a Higgs boson and a W boson," Tech. Rep. CMS-PAS-SUS-20-003, CERN, Geneva, 2021. https://cds.cern.ch/record/2758360.

[260] ATLAS Collaboration, "Search for electroweak production of charginos and sleptons decaying into final states with two leptons and missing transverse momentum in $\sqrt{s}$ = 13 TeV pp collisions using the ATLAS detector," *Eur. Phys. J. C* **80** (2020) 123, arXiv:1908.08215 [hep-ex].

[261] G. Apollinari, I. Béjar Alonso, O. Brüning, *et al.*, *High-Luminosity Large Hadron Collider (HL-LHC): Preliminary Design Report*. CERN Yellow Reports: Monographs. CERN, Geneva, 2015. https://cds.cern.ch/record/2116337.

[262] X. Chen, S. Dallmeier-Tiessen, R. Dasler, *et al.*, "Open is not enough," *Nature Physics* **15** no. 2, (Feb, 2019) 113–119. https://doi.org/10.1038/s41567-018-0342-2.

[263] LHC Reinterpretation Forum Collaboration, W. Abdallah *et al.*, "Reinterpretation of LHC Results for New Physics: Status and Recommendations after Run 2," *SciPost Phys.* **9** no. 2, (2020) 022, arXiv:2003.07868 [hep-ph].

[264] ATLAS Collaboration, "RECAST framework reinterpretation of an ATLAS Dark Matter Search constraining a model of a dark Higgs boson decaying to two b-quarks." ATL-PHYS-PUB-2019-032, 2019. https://cds.cern.ch/record/2686290.

[265] K. Cranmer and I. Yavin, "RECAST: Extending the Impact of Existing Analyses," *JHEP* **04** (2011) 038, arXiv:1010.2506 [hep-ex].

[266] D. Dercks, N. Desai, J. S. Kim, *et al.*, "CheckMATE 2: From the model to the limit," *Comput. Phys. Commun.* **221** (2017) 383–418, arXiv:1611.09856 [hep-ph].

[267] M. Drees, H. Dreiner, D. Schmeier, *et al.*, "CheckMATE: Confronting your Favourite New Physics Model with LHC Data," *Comput. Phys. Commun.* **187** (2015) 227–265, arXiv:1312.2591 [hep-ph].

[268] E. Conte, B. Fuks, and G. Serret, "MadAnalysis 5, A User-Friendly Framework for Collider Phenomenology," *Comput. Phys. Commun.* **184** (2013) 222–256, arXiv:1206.1599 [hep-ph].

[269] E. Maguire, L. Heinrich, and G. Watt, "HEPData: a repository for high energy physics data," *J. Phys. Conf. Ser.* **898** no. 10, (2017) 102006, arXiv:1704.05473 [hep-ex].

[270] ATLAS Collaboration, "Simpleanalysis." https://gitlab.cern.ch/atlas-sa/simple-analysis, 2021.

[271] S. Ovyn, X. Rouby, and V. Lemaitre, "DELPHES, a framework for fast simulation of a generic collider experiment," arXiv:0903.2225 [hep-ph].

[272] A. Buckley, J. Butterworth, D. Grellscheid, *et al.*, "Rivet user manual," *Comput. Phys. Commun.* **184** (2013) 2803–2819, arXiv:1003.0694 [hep-ph].

[273] A. Buckley, D. Kar, and K. Nordström, "Fast simulation of detector effects in Rivet," *SciPost Phys.* **8** (2020) 025, arXiv:1910.01637 [hep-ph].

[274] S. Kraml, S. Kulkarni, U. Laa, *et al.*, "SModelS: a tool for interpreting simplified-model results from the LHC and its application to supersymmetry," *Eur. Phys. J. C* **74** (2014) 2868, arXiv:1312.4175 [hep-ph].

[275] F. Ambrogi, S. Kraml, S. Kulkarni, *et al.*, "SModelS v1.1 user manual: Improving simplified model constraints with efficiency maps," *Comput. Phys. Commun.* **227** (2018) 72–98, arXiv:1701.06586 [hep-ph].

[276] ATLAS Collaboration, "Search for direct production of electroweakinos in final states with one lepton, missing transverse momentum and a higgs boson decaying into two b-jets in pp collisions at $\sqrt{s}$ = 13 tev with the atlas detector," 2021. https://www.hepdata.net/record/ins1755298?version=4.

[277] ATLAS Collaboration, "1lbb-likelihoods-hepdata.tar.gz," 2020. https://www.hepdata.net/record/resource/1408476?view=true.

[278] G. Alguero, S. Kraml, and W. Waltenberger, "A SModelS interface for pyhf likelihoods," arXiv:2009.01809 [hep-ph].

[279] M. D. Goodsell, "Implementation of the ATLAS-SUSY-2019-08 analysis in the MadAnalysis 5 framework (electroweakinos with a Higgs decay into a $b\bar{b}$ pair, one lepton and missing transverse energy; 139 fb^{-1})," *Mod. Phys. Lett. A* **36** no. 01, (2021) 2141006.

[280] J. Y. Araz *et al.*, "Proceedings of the second MadAnalysis 5 workshop on LHC recasting in Korea," *Mod. Phys. Lett. A* **36** no. 01, (2021) 2102001, arXiv:2101.02245 [hep-ph].

[281] M. Feickert, L. Heinrich, G. Stark, and B. Galewsky, "Distributed statistical inference with pyhf enabled through funcX," in *25th International Conference on Computing in High-Energy and Nuclear Physics*. 3, 2021. arXiv:2103.02182 [cs.DC].

[282] R. Chard, Y. Babuji, Z. Li, *et al.*, "funcx: A federated function serving fabric for science," ACM, Jun, 2020. http://dx.doi.org/10.1145/3369583.3392683.

[283] D. Merkel, "Docker: Lightweight linux containers for consistent development and deployment," *Linux J.* **2014** no. 239, (Mar., 2014) .

[284] S. Binet and B. Couturier, "docker & HEP: Containerization of applications for development, distribution and preservation," *J. Phys.: Conf. Ser.* **664** no. 2, (2015) 022007. 8 p. https://cds.cern.ch/record/2134524.

[285] K. Cranmer and L. Heinrich, "Yadage and Packtivity - analysis preservation using parametrized workflows," *J. Phys. Conf. Ser.* **898** no. 10, (2017) 102019, arXiv:1706.01878 [physics.data-an].

[286] E. R. Gansner and S. C. North, "An open graph visualization system and its applications to software engineering," *SOFTWARE - PRACTICE AND EXPERIENCE* **30** no. 11, (2000) 1203–1233.

[287] E. R. Gansner, Y. Koren, and S. North, "Graph drawing by stress majorization," in *Graph Drawing*, J. Pach, ed., pp. 239–250. Springer Berlin Heidelberg, Berlin, Heidelberg, 2005.

[288] ATLAS Collaboration, "Electron and photon energy calibration with the ATLAS detector using 2015–2016 LHC proton–proton collision data," *JINST* **14** (2019) P03017, arXiv:1812.03848 [hep-ex].

[289] Schanet, Eric, "simplify," Version 0.1.5. https://github.com/eschanet/simplify.

[290] Schanet, Eric, "SUSY-2019-08 simplified likelihood," Version 0.0.1. https://github.com/eschanet/simplify/blob/master/examples/ANA-SUSY-2019-08/simplify_BkgOnly.json.

[291] P. C. Bryan and M. Nottingham, "Javascript object notation (json) patch," Version RFC 6902, Apr, 2013. https://www.rfc-editor.org/rfc/rfc6902.txt.

[292] ATLAS Collaboration, "Search for direct stau production in events with two hadronic τ-leptons in $\sqrt{s} = 13$ TeV pp collisions with the ATLAS detector," *Phys. Rev. D* **101** (2020) 032009, arXiv:1911.06660 [hep-ex].

[293] ATLAS Collaboration, "Search for bottom-squark pair production with the ATLAS detector in final states containing Higgs bosons, b-jets and missing transverse momentum," *JHEP* **12** (2019) 060, arXiv:1908.03122 [hep-ex].

[294] W. Porod, "SPheno, a program for calculating supersymmetric spectra, SUSY particle decays and SUSY particle production at e+ e- colliders," *Comput. Phys. Commun.* **153** (2003) 275–315, arXiv:hep-ph/0301101.

[295] W. Porod and F. Staub, "SPheno 3.1: Extensions including flavour, CP-phases and models beyond the MSSM," *Comput. Phys. Commun.* **183** (2012) 2458–2469, arXiv:1104.1573 [hep-ph].

[296] S. Heinemeyer, W. Hollik, and G. Weiglein, "FeynHiggs: A Program for the calculation of the masses of the neutral CP even Higgs bosons in the MSSM," *Comput. Phys. Commun.* **124** (2000) 76–89, arXiv:hep-ph/9812320.

[297] H. Bahl, T. Hahn, S. Heinemeyer, *et al.*, "Precision calculations in the MSSM Higgs-boson sector with FeynHiggs 2.14," *Comput. Phys. Commun.* **249** (2020) 107099, arXiv:1811.09073 [hep-ph].

[298] T. Hahn, S. Heinemeyer, W. Hollik, *et al.*, "High-Precision Predictions for the Light CP -Even Higgs Boson Mass of the Minimal Supersymmetric Standard Model," *Phys. Rev. Lett.* **112** no. 14, (2014) 141801, arXiv:1312.4937 [hep-ph].

[299] B. C. Allanach, "SOFTSUSY: a program for calculating supersymmetric spectra," *Comput. Phys. Commun.* **143** (2002) 305–331, arXiv:hep-ph/0104145 [hep-ph].

[300] G. Belanger, F. Boudjema, A. Pukhov, and A. Semenov, "MicrOMEGAs 2.0: A Program to calculate the relic density of dark matter in a generic model," *Comput. Phys. Commun.* **176** (2007) 367–382, arXiv:hep-ph/0607059.

[301] G. Belanger, F. Boudjema, A. Pukhov, and A. Semenov, "micrOMEGAs: A Tool for dark matter studies," *Nuovo Cim. C* **033N2** (2010) 111–116, arXiv:1005.4133 [hep-ph].

[302] W. Beenakker, R. Hopker, and M. Spira, "PROSPINO: A Program for the Production of Supersymmetric Particles in Next-to-leading Order QCD," Tech. Rep. hep-ph/9611232, Nov, 1996. https://cds.cern.ch/record/314229. 12 pages, latex, no figures, Complete postscript file and FORTRAN source codes available from http://wwwcn.cern.ch/ mspira/prospino/.

[303] W. Beenakker, M. Klasen, M. Kramer, *et al.*, "The Production of charginos / neutralinos and sleptons at hadron colliders," *Phys. Rev. Lett.* **83** (1999) 3780–3783, arXiv:hep-ph/9906298. [Erratum: Phys.Rev.Lett. 100, 029901 (2008)].

[304] ATLAS Collaboration, "Search for long-lived charginos based on a disappearing-track signature using 136 fb^{-1} of pp collisions at $\sqrt{s}$ = 13 TeV with the ATLAS detector," Tech. Rep. ATLAS-CONF-2021-015, CERN, Geneva, Mar, 2021. https://cds.cern.ch/record/2759676.

[305] A. Arbey, M. Battaglia, and F. Mahmoudi, "Higgs Production in Neutralino Decays in the MSSM - The LHC and a Future e^+e^- Collider," *Eur. Phys. J. C* **75** no. 3, (2015) 108, arXiv:1212.6865 [hep-ph].

[306] M. E. Cabrera, J. A. Casas, A. Delgado, *et al.*, "Naturalness of MSSM dark matter," *JHEP* **08** (2016) 058, arXiv:1604.02102 [hep-ph].

[307] N. Arkani-Hamed, G. L. Kane, J. Thaler, and L.-T. Wang, "Supersymmetry and the LHC inverse problem," *JHEP* **08** (2006) 070, arXiv:hep-ph/0512190.

[308] S. Amari, *Differential-Geometrical Methods in Statistics.* Springer New York, New York, NY, 1985.

[309] J. Brehmer, K. Cranmer, F. Kling, and T. Plehn, "Better Higgs boson measurements through information geometry," *Phys. Rev. D* **95** no. 7, (2017) 073002, arXiv:1612.05261 [hep-ph].